

**DEVELOPMENT OF AN IN-SITU DETECTOR FOR DISSOLVED GASES IN LIQUID
WASTE**

by

Ali Davoodabadi Farahani

B.Sc., K. N. Toosi University of Technology, 2017

A THESIS SUBMITTED IN PARTIAL FULFILLMENT OF
THE REQUIREMENTS FOR THE DEGREE OF

MASTER OF APPLIED SCIENCE

in

THE COLLEGE OF GRADUATE STUDIES

(Mechanical Engineering)

THE UNIVERSITY OF BRITISH COLUMBIA

(Okanagan)

April 2021

© Ali Davoodabadi Farahani, 2021

The following individuals certify that they have read, and recommend to the College of Graduate Studies for acceptance, a thesis/dissertation entitled:

DEVELOPMENT OF AN IN-SITU DETECTOR FOR DISSOLVED GASES IN
LIQUID WASTE

submitted by Ali Davoodabadi Farahani in partial fulfillment of the requirements of the degree of Master of Applied Science.

Dr. Mina Hoorfar, School of Engineering

Supervisor

Dr. Homayoun Najjaran, School of Engineering

Supervisory Committee Member

Dr. Chen Feng, School of Engineering

Supervisory Committee Member

Dr. Ray Taheri, School of Engineering

University Examiner

Abstract

Monitoring volatile compounds in sewer systems is highly important due to the toxic and corrosive nature of various nuisance chemicals generated, such as hydrogen sulfide (H_2S). Hotspot monitoring facilitates identification of the location of the generated H_2S , and thereby targeted treatment can be applied, which eventually minimizes the use of chemicals and lowers the environmental effect within the sewer system. In this thesis, we present a portable detector that is designed to extract volatile components from aqueous samples by vaporizing the sample and then exposing it to a microfluidic-based detector, fabricated by a selective microchannel embedded with a metal oxide semiconductor (MOS) sensor. The setup consists of an exposure and recovery chamber, heater, servo, and a peristaltic liquid pump. The entire device is controlled using a microcomputer that transmits sensor data and receives inputs from the user. A testing procedure is also established for the setup, which consists of 5 steps, including sample extraction, vaporization, exposure, recovery, and purging. Using a wide concentration ranges of H_2S and ammonia (NH_3) dissolved in water (i.e., two components which the MOS sensor has potential cross-selectivity), a database for classification and regression was developed: the device was capable of classifying between NH_3 and H_2S by a recall value of 100% and 96% in separate and also returned a recall value of 97% with H_2S classification and 96% with NH_3 classification in mixture aqueous solutions. Regression precision for separate and mixture aqueous solutions was 84.6% and 88.77%, respectively. The developed setup was used in a field test (at Annacis Island (Delta, BC) wastewater treatment plant (AI-WWTP)) where various tasks such as sample extraction, evaporation, and data transmission were automatically performed. The results show that the device is capable of identifying and measuring the concentration of H_2S and NH_3 in raw influent with

83.48% precision. Overall, the results presented show the potential of the proposed automated wireless device in recognizing and measuring NH_3 and H_2S in sewer systems which can facilitate the detection of hotspots, reduction of treatment costs, increase of the lifespan of buried infrastructure, and minimization of the involvement of highly-skilled personnel.

Lay summary

In this study, a portable device was designed to automatically measure the amount of toxic and corrosive substances in the sewer network. The output of the device facilitates the decision-making process in terms of the amount of chemicals needed to be injected into the system for treatment purposes. This will lead to a decrease in the maintenance costs of the sewer infrastructure and improve the safety of plant workers. To ensure the functionality of the designed prototype, it was taken to wastewater facilities and tested in real working conditions. The results have been very promising, showing the potential of this device for commercialization. The success and benefits of this project can be easily translated to other public utilities across Canada and international communities.

Preface

The provided research in this thesis is the original work performed by the author and supervised by Dr. Mina Hoorfar at the Advanced Thermofluidic Laboratory (ATFL) at the School of Engineering, University of British Columbia. The details of publications and the author's contributions to them are explained below:

a. Journal publications

A. Davoodabadi Farahani, J. A. T Hunter, G. P. McIntosh, E. Earl, A. Ravishankara, N. Tasnim, P. Kadota, M. Hoorfar, "Development of an in-situ detector for dissolved gases in liquid waste," submitted to *Sensors and Actuators, B: Chemical* (April 2021)

Contribution: My contribution in this paper included the following: (i) conducting the experiments, (ii) developing the setup, and (iii) writing the paper

b. Conference proceedings and presentations

A. Yavarinasab, S. Janfaza, M. Mohaghegh Montazeri, N. Tasnim, A. Davoodabadi Farahani, P. Kadota, P. Markin, Arash Dalili, E. Taatizadeh, H. Tahmooressi, M. Hoorfar, "A graphene-based chemical sensor for hydrogen sulfide measurement in water," 2019 IEEE SENSORS, Montreal, QC, Canada.

Contribution: My contribution in this paper included the following: (i) defining the strategies and (ii) editing the paper.

Table of contents

Abstract.....	iii
Lay summary	v
Preface.....	vi
Table of contents.....	vii
List of tables.....	x
List of figures.....	xi
1 Introduction.....	1
1.1 Overview.....	1
1.2 Literature review.....	3
1.2.1 H ₂ S in sewer environment	3
1.2.2 Treatment methods.....	5
1.2.3 Sensors for measurement of H ₂ S	8
1.2.3.1 Electrochemical sensors	10
1.2.3.2 Optical sensors.....	10
1.2.3.3 Piezoelectric sensors.....	11
1.2.3.4 Metal oxide semiconductor sensors.....	12
1.2.3.5 MEMS sensors.....	13
1.2.3.6 Nano-structured sensors	14
1.2.3.7 Sensors from organic or inorganic nanomaterials	14
1.2.4 Review of integrated devices	15
1.3 Motivation.....	20
1.4 Objectives	20

1.5	Organization of thesis	21
2	Experimental setup.....	22
2.1	Microfluidic-based detector	22
2.2	Benchtop setups	24
2.2.1	Version 1	24
2.2.2	Version 2.....	27
2.2.2.1	Sensor arrangement	28
2.2.2.2	Vaporization chamber and heater	31
2.2.2.3	Sample delivery system.....	36
2.2.2.4	Purging system and filtration.....	37
2.2.2.5	Testing procedure and data capture	39
3	Results of individual gases.....	42
3.1	Consistency and longevity tests	42
3.2	Characterizing tests.....	43
3.3	Ammonia results	45
3.3.1	Classification and regression	45
3.4	Discussion.....	47
4	Mixture results	48
4.1	H ₂ S and NH ₃ mixture.....	48
4.2	Classification and regression	50
4.3	Field Test	51
5	Summary, contributions, and future works.....	53
5.1	Summary.....	53

5.2	Contributions.....	54
5.3	Future works	54
6	References.....	56

List of tables

Table 1.1 Summary of available devices for H₂S measurement..... 19

List of figures

Figure 1.1 Mechanism of concrete corrosion. (reprinted from [23] with permission from Springer Nature)	5
Figure 1.2 H ₂ S control methods in the sewer environment. (reprinted from [3] with permission from Elsevier)	8
Figure 1.3 Common sensor types for real-time detection of H ₂ S gas. (reprinted from [55] with permission from Elsevier).....	9
Figure 1.4 Online dissolved sulfide monitoring system and its field installation. (reprinted from [6] with permission from Elsevier).....	18
Figure 2.1 The Selective microfluidic system embedded with a MOS sensor	22
Figure 2.2 Schematic of the detector showing the channel, coatings, and the gas molecules diffusing through the channel (reprinted from [107] with permission from IEEE)..	23
Figure 2.3 Sensor's housing	25
Figure 2.4 Version 1 prototype device: (a) major components include a rechargeable power source, touch-controlled graphical user interface, sample vaporization, and gas sensing modules; (b) key internal components for automated sample extraction.	25
Figure 2.5 The jar configuration including the microfluidic-based detector and the vaporization chamber.....	26
Figure 2.6 Version 2 (Outside configuration).....	27
Figure 2.7 Version 2 (inside configuration): A - Protoboard, B - Raspberry Pi, C, and D - Purging valves, E - Peristaltic pump, F - Battery, G - Purging pump, H –Microfluidic-based detector, I - Exposure and recovery valve.	28
Figure 2.8 The designed potentiostatic circuit to replace the VersaSTAT 4.....	30

Figure 2.9 MOS and electrochemical sensor arrangement on an uncoated 3D printed dual channel detector.....	30
Figure 2.10 Corroded magnet in Version 1.	31
Figure 2.11 Magnets inside the jar configuration in Version 1.	32
Figure 2.12 The porcelain crucible inside the vaporization chamber.	33
Figure 2.13 Exposure and recovery chambers section view.	34
Figure 2.14 Exposure and recovery valve motor comparison.	35
Figure 2.15 The new heating element with the 3D printed container.	35
Figure 2.16 The final design of vaporization chamber and heater.	36
Figure 2.17 Adafruit peristaltic liquid pump with silicone tubing.....	37
Figure 2.18 Filter arrangement.	38
Figure 2.19 Purging inlets and outlets.	38
Figure 2.20 The graphical user interface in Version 1.....	40
Figure 2.21 Main window of the graphical user interface.	40
Figure 2.22 Manual controls of the interface.....	41
Figure 2.23 Long-run test's user interface.	41
Figure 3.1 The response of two TGS 2602 sensors being exposed to a similar sample. The first three curves are for the first three tests and the last curve shows the 23 rd test (last test).	43
Figure 3.2 Detector response to H ₂ S dissolved in water. The inset shows responses to water and low H ₂ S concentrations.....	44
Figure 3.3 Comparing detector response to ammonia and hydrogen sulfide present individually in aqueous samples.....	45

Figure 4.1 Increasing NH₃ concentration from 18 to 29 mg/l at a constant level of H₂S at 10 mg/l.
..... 48

Figure 4.2 Increasing NH₃ concentration from 18 to 29 mg/l at a constant level of H₂S at 20 mg/l.
..... 49

Figure 4.3 Increasing H₂S concentration from 10 to 20 mg/l at a constant level of NH₃ at 18 mg/l.
..... 49

Figure 4.4 Increasing H₂S concentration from 10 to 20 mg/l at a constant level of NH₃ at 29 mg/l.
..... 50

Figure 4.5 Version 2 running continuous experiments at Annacis island Research Center. 52

Figure 4.6 Field test responses for raw influent..... 52

1 Introduction

1.1 Overview

Wastewater collection and treatment are indispensable public services to maintain clean waterways and protect public health. Sewage systems create a suitable environment for microbial activity, in which a variety of nuisance gases and malodorous compounds are produced. In addition to being hazardous, noxious chemicals produced in the sewer environment, such as hydrogen sulfide (H_2S), have corrosiveness characteristics which can ultimately result in infrastructure failure and gas leakage, requiring millions of dollars to repair every year. Pipe corrosion and biogenic gas generation also cause the flow of unpleasant odor into pump stations, channels, ducts, and manholes which are hugely concerned in metropolitan regions [1].

Although different strategies are available to mitigate biogenic nuisance gases, they will perform more effectively if specific data is available for identifying “hotspots” of gas formation for targeted treatment [2]. Furthermore, based on the biogenic gas concentration level, the sewer system should undergo a different mitigation method (e.g., the addition of biocides, iron salts, chemical oxidants, etc.) [3]. Therefore, there is a huge demand in wastewater industries for an automated, real-time, in-situ detector capable of detecting multiple target compounds which are dissolved in sewerage. Current liquid-phase monitoring apparatuses are expensive and difficult to operate as they clog quickly and require high maintenance. Since current technologies have a few limitations (like the large footprint, low precision and reliability, and incapable of liquid-phase analysis), there is an urgent need for a suitable detector that overcomes all of these restrictions [4]–[7]. The importance of detecting target analytes in the liquid phase is because (i) the gas concentration within the

headspace along the sewer pipeline might not be identical, and (ii) it is essential to detect noxious gas formation in anaerobic biofilms at the “hotspots” where analytes have not turned into the gaseous phase during their biogenic activity. As for the former, gas-phase readings of H₂S concentrations can be highly variable, which makes the analysis and control of odor mitigation solutions challenging. On the other hand, the measurement of H₂S dissolved in wastewater can provide greater reading stability and better control over odor-reducing agents. As for the latter reason, diminutive amounts of dissolved nuisance gases (e.g., H₂S) in sewage can create a high concentration of hydrogen sulfide within the headspace (> 100 ppm) [2].

The overall research goal of this study is to design, develop, prototype, and evaluate a robust in-situ sensor technology to measure H₂S dissolved in wastewater and to help mitigate H₂S “hotspots.” To achieve the proposed goal, a core microfluidic-based gas sensing technology that detects H₂S from a vaporized liquid effluent sample is developed using a metal oxide semiconductor (MOS) and a 3D printed microfluidic diffusion channel. A purging and recovery process is also designed for each test to ensure the device is rapidly restored between experiments. The sensor is then integrated into a vaporization and recovery chamber which are linked to a sample extraction and delivery system. Liquid samples obtained from the sewer lines pass through a peristaltic pump for extracting the required amount of the sample prior to vaporization and exposure to the sensing unit. A microcontroller and data collection components are utilized to monitor and ensure all components are operating properly and can transmit and analyze data through an application on the portable device. Also, the most suitable method to install the device within sewerage pipes is determined in a field test which guides design requirements to develop a robust platform to integrate and maintain the components for long runs.

Similar to any other sensor, calibration is an important step to convert the collected raw data to the desired output. Every response obtained from the detector needs to reflect a certain concentration. The proposed microfluidic-based gas detector is calibrated using liquid chromatography-mass spectrometry (LC-MS) for responses in liquid concentrations. LC-MS data are basically listing the composition and proportions of dissolved target analytes in liquid waste samples.

The sensor used in the setup requires training in order to recognize a particular “smell print” of target gases in a given liquid waste sample. The selectivity of the device is defined as the ability of the system to differentiate between different analytes (in particular, H_2S and NH_3). A pattern recognition software is used to analyze each curve acquired from exposing samples to the detector. Using datasets from testing a wide concentration range of H_2S and NH_3 in the liquid phase are used as input to a machine learning algorithm which outputs the presence and the concentration of hydrogen sulfide and ammonia (two components in sewer samples which the MOS sensor has potential cross-selectivity). This eventually provides the ability to detect and differentiate different compounds in sewage and estimates the concentration of that target gas in the surrounding liquid environment.

1.2 Literature review

1.2.1 H_2S in the sewer environment

Wastewater within sewer pipes creates an excellent medium for the biological production of nuisance gases (such as H_2S). The formation of noxious gases can cause corrosion within the pipes and eventually leads to infrastructural failure. H_2S is a known odorous and hazardous material due to its toxicity [8], [9]. Apart from its harmful impact on the environment and unpleasant odor, it

can be detrimental or even lethal to living organisms at relatively low concentrations. The normal “rotten egg” smell of H_2S can be sensed by the human olfactory system at concentrations of 0.02 to 0.13 ppm [8], yet concentrations around 80 ppm cause a severe olfactory neuron loss in rats [10]. At the exposure level of 500 to 1000 ppm, it causes dizziness, olfactory paralysis, and/ or immediate death [11].

Wastewater is full of organic materials and sulphate. Since the sewage environment is a closed system, oxygen availability is limited. In this condition, microorganisms (like proteolytic bacteria such as *Desulfovibrio* and *Desulfobulbus*, which are sulphate-reducing bacteria (SRB)) form hydrogen sulphide (H_2S) as well as carbon dioxide (CO_2) within a hydrolytic reaction of protein from organic sulfur compounds [12]. The generation of H_2S in an anaerobic condition by the sulfate reducing bacteria (SRB) is controlled by the sulfate concentration, pH level, and oxygen availability [13]–[15]. However, the produced H_2S does not destruct concrete pipes. It escapes from the liquid phase into the headspace and dissolves in the slime layer (biofilm) at the crown of pipes above the liquid level. The H_2S deposited into the slime at the headspace is oxidized by the sulfur oxidizing bacteria (SOB) (which are basically from the *Thiobacillus* genus [16]–[18]) in an aerobic condition, and sulfuric acid (H_2SO_4) is formed as a product of this reaction. Thus, the produced H_2S in wastewater pipes indirectly contributes to the corrosion of pipes by producing sulfuric acid (H_2SO_4). In summary, the above reactions occur in 4 steps: firstly, SRB reduces sulphate to sulphide; secondly, H_2S escapes to headspace and biofilm; thirdly, SOB oxidizes and turns sulphide into H_2SO_4 , and finally, concrete is corroded by the sulfuric acid. All reactions are summarized in Figure 1.1. CO_2 also evaporates and reacts with moisture and creates carbonic acid (H_2CO_3), which eventually leads to the carbonation of concrete [19].

In sewerage pipes, corrosion does not occur if the pipes are running with a full flow. It only happens when there is room for H₂S to diffuse and escape to the crown of the pipe (i.e., the headspace) [20]. Annually, sewer pipes are corroded 0.08-10 mm by H₂SO₄ generation [21]. If the total dissolved sulfide in liquid is in the range of 0.1 mg/L, corrosion and if it is more than 2 mg/L, extreme corrosion of the concrete pipe will occur [22].

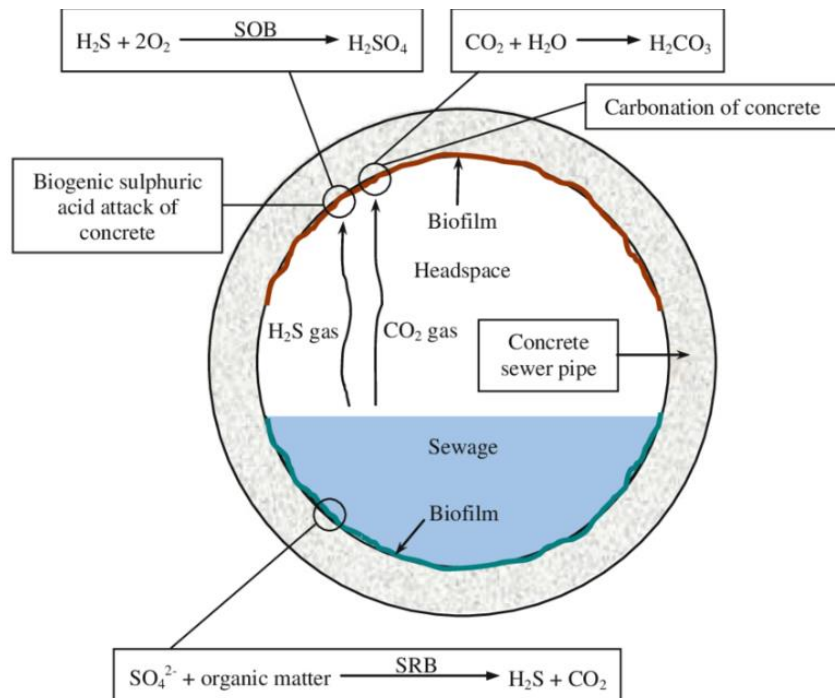


Figure 1.1 Mechanism of concrete corrosion (reprinted from [23] with permission from Springer Nature)

1.2.2 Treatment methods

Biologically induced corrosion of liquid waste infrastructure can extremely decrease its lifespan and present a loss in the asset value in the order of hundreds of millions of dollars. In Greater Vancouver, the wastewater system manages the liquid waste of approximately 2 million people, which makes up to 1 billion liters of liquid waste every day. The estimated cost of such failures in

Metro Vancouver is known to be in the magnitude of billions of dollars [24], [25]. A variety of methods have been utilized to address these concerns. Several controlling strategies have been implemented to manage the harmful impact of H₂S and subsequent H₂SO₄ generation. These strategies include sewer pipe redesigning [26], [27], employing protective pipeline coatings [28], [29], treatment filters to control malodorous compounds [30], [31], using more resistant materials in pipes [32]–[34] and restricting H₂S formation and corrosion [3], [35]–[37]. Hence, the relatively high cost associated with wastewater reconstruction and modification makes direct targeting sites of high SRB activity a viable option in maintaining sewer infrastructure and mitigating both health and environmental impacts by preventing noxious gas release [38].

Among current treatment methods employed to inhibit H₂S generation or eliminate formed H₂S, increasing redox potential is favorable to control hydrogen sulfide formation. Dissolving oxygen or air can prevent sulfide generation [39]–[42]. Generally, high dissolved oxygen (DO) levels of 0.5 mg/L are required. Air injection has a limited capacity in transferring oxygen (DO levels of 3–5 mg/L), while pure oxygen can increase DO level to 5–7 mg/L, which is more effective. Pure oxygen injection is mostly beneficial in high-pressure sewage systems, but it increases fire risks [43]. An addition of oxidizing chemicals including hydrogen peroxide (H₂O₂) [38], chlorine in gas or aqueous solutions (NaClO or Ca(ClO)₂) [38], [44], potassium permanganate (KMnO₄) [38], and nitrate [45] is another method used to mitigate H₂S formation. However, the associated cost with chemical dosing is high; for example, H₂O₂ and chlorine addition will cost between \$2.9 – 6.41 kg⁻¹S, and potassium permanganate sits at around \$28.81 – 33.53 kg⁻¹S [3].

Precipitation of metal sulfides also reduces dissolved sulfide from sewerage. Iron, due to its impact in managing the concentration of sulfides dissolved in sewage, has been normally used in sewer

systems [22], [46], [47]. Ferrous chloride (FeCl_2) [48], iron (II) sulfate (FeSO_4) [49], and ferric nitrate ($\text{Fe}(\text{NO}_3)_3$) [50] can be added to wastewater for removing sulfide (by precipitating) and producing ferrous sulfide (FeS) [3]. It has been observed that the precipitation of ferrous sulfide can take a few hours with iron salts of chloride [48]. Moreover, biocides and molybdate can inhibit H_2S production since they can inhibit biological activity [51]–[53]. pH elevation by adding sodium hydroxide (NaOH) can also inhibit biological activity by preventing the releasing of the H_2S gas release when pH is more than 9 or inactivating SRB when pH is in the range of 12.5 – 13 [3]. The summary of chemical dosing technologies and biological methods is presented in Figure 1.2. The downsides of the aforementioned methods include the expensive and high amount of required chemicals for long-time use, and potential unsafe handling, and related environmental issues. These issues suggest the use of chemicals in wastewater networks as low as possible. This factor increases the importance of having a robust monitoring system capable of reporting the available amount of H_2S in wastewater lines and subsequently SRB activity to increase the efficiency in detection of hotspots and H_2S formation points along the pipe and eventually decreasing the cost of treatments in the infrastructure by reducing corrosion caused by H_2S generation.

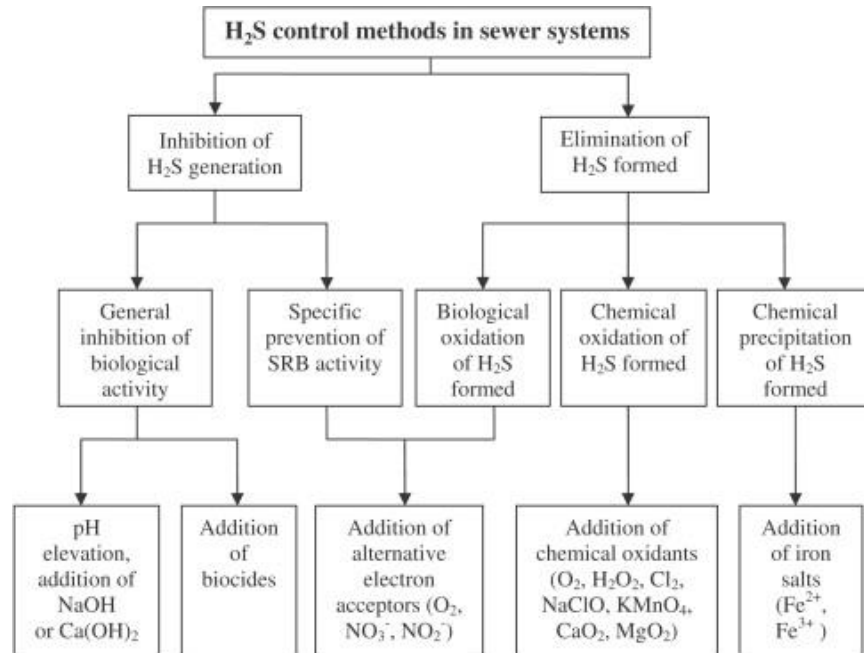


Figure 1.2 H₂S control methods in the sewer environment. (reprinted from [3] with permission from Elsevier)

1.2.3 Sensors for measurement of H₂S

Current H₂S gas sensors are relatively costly (\$100- \$1000) and require high power, have a poor limit of detection, instability, and inflexibility, to name a few [54]. So far, numerous technologies have been utilized for H₂S sensing (Figure 1.3) [55]. Electrochemical-based sensors have been used since the 1950s; however, they have limitations, including low selectivity, high operational temperature, sensitivity to the pressure change, and short stability period. Optical sensing technologies have developed expeditiously since 1977. However, due to limitations like large size, low selectivity, limited operational temperature, and high cost, their usage as gas sensors are restricted. Since 1880, the piezoelectric effect was used as a sensing method however the sensors developed based on this effect suffer from high operational temperature, small output signal (voltage) and relatively high noise (due of the dimension reduction that causes instability when surface to volume ratio increases). Since fifty years ago, metal oxide semiconductors have shown

excellent potentials in H₂S detection due to their physical properties (i.e., a large surface to volume ratio in the nanostructure especially inorganic tungsten oxide (WO₃) nanoparticles). In the following subsections each of these sensing mechanisms are reviewed thoroughly.

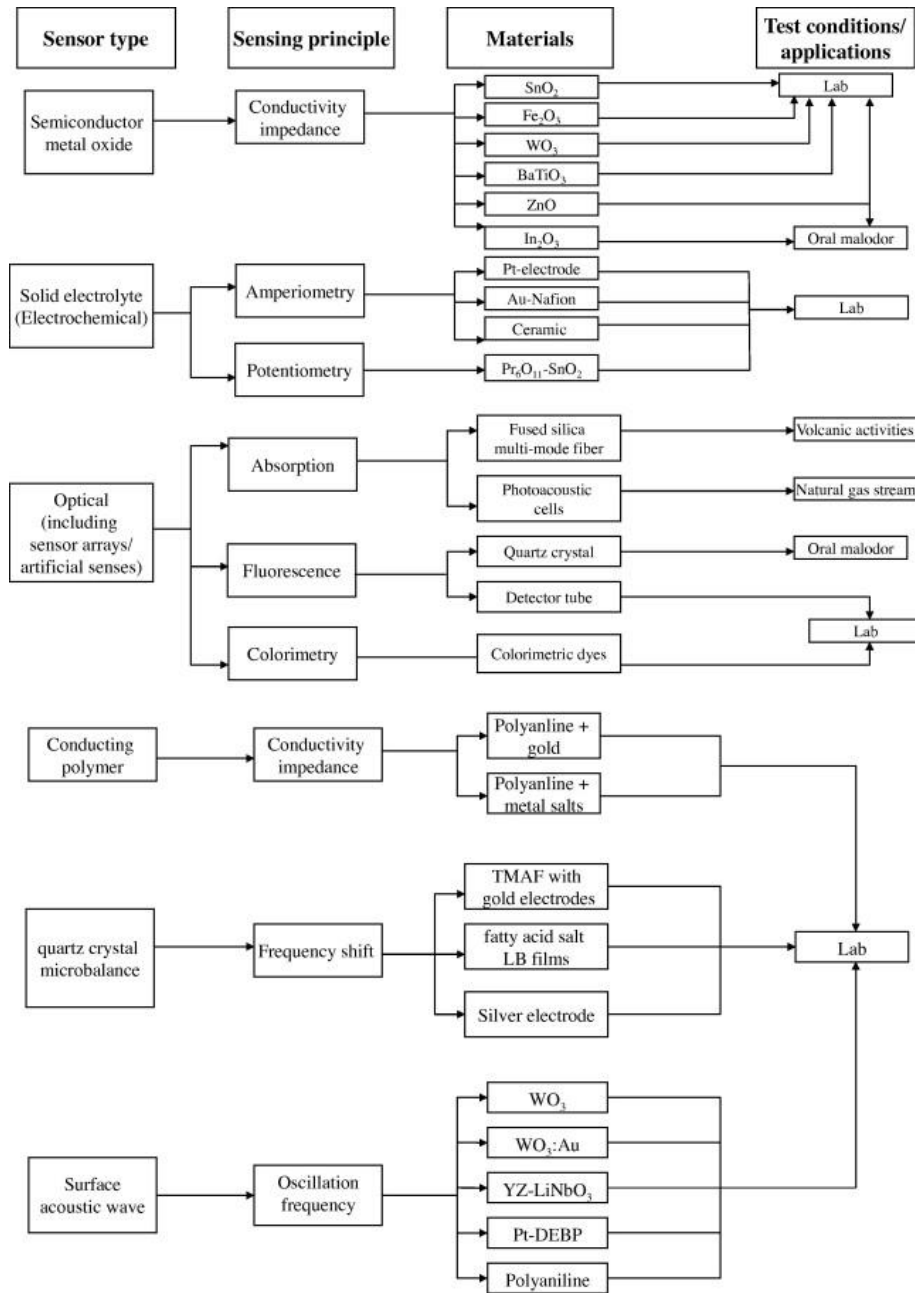


Figure 1.3 Common sensor types for real-time detection of H₂S gas. (reprinted from [55] with permission from Elsevier)

1.2.3.1 Electrochemical sensors

Electrochemical sensors are based on solid or liquid electrolytes. They generate an electrical signal once they are exposed to gas; the signal is proportional to the gas concentration. Based on the signal, the sensor can be either amperometric or potentiometric. For the former, the rate of electron transfer (current) as a function of time is proportional to the target compound's concentration (based on Faraday's law and mass transport phenomena). In the case of the latter, ion-selective electrodes are used to have a potential signal that is proportionate to the concentration logarithmically [56], [57]. An example of solid electrolyte potentiometric sensor is reported in the work of by Liang et al. [58]: they used sodium super ionic conductor (NASICON) and Pr_6O_{11} - doped SnO_2 electrodes for H_2S detection in a range of 5 – 50 ppm and a response time within 4 – 8 s with a noble resistance to water vapor. Another example of the solid electrolyte sensors is H_2SO_4 pre-treated Nafion membrane coated with Au catalyst for selectivity improvement toward H_2S sensing. The detection range of 1–100 ppm with 0.1 ppm detectability in a 9-s response was achieved [59]. However, commercially available solid electrolyte sensors have limitations, including selectivity, operational temperature, pressure change sensitivity, and short maintenance period. Also, chemical interference of H_2S gas sometimes causes false readings [60], [61].

1.2.3.2 Optical sensors

Measurements are based on the interactions among light and the analyte within the fiber and thin-film coating, which sensing occurs via absorption and emission spectroscopy technique. In most optical sensors, measurement is conducted directly. Examples include, mid-infrared sensors [62], direct ultraviolet spectrophotometric sensors [63], laser-based sensors [64], Fourier transform infrared spectrometry (FTIR) based sensors [65], and non-dispersive infrared (NDIR) gas analysis

[66]. An example of a direct sensing method is the research carried out by Vagra et al. [67] in which a dual-channel photoacoustic spectroscopy system was introduced. They used a single-mode, fiber-coupled, room-temperature-operated, telecommunication-type diode laser to detect H₂S as low as 0.5 ppm. The application of these sensors is restricted due to the high cost and complexity [54].

1.2.3.3 Piezoelectric sensors

This sensing technique is more popular in industries including aerospace, automotive, and energy due to its high operating temperature (>800 °C) [68]. These sensors are either surface acoustic wave (SAW) or Quartz Crystal Microbalance (QCM), and their measurement is based on mass changes. Different materials have been used in piezoelectric sensors (such as gallium phosphate (GaPO₄), lithium niobate (LiNbO₃), langasite (La₃Ga₅SiO₁₄), silicon dioxide (SiO₂), and aluminum nitride (AlN) [54]). SAW sensors are either based on the Rayleigh wave movement over its superficies or the mass change which causes the oscillation frequency change. Jakubik et al. [69] used Polyaniline thin films for SAW H₂S sensor in synthetic dry air in which the resulted sensor showed a detectability range of 25–500 ppm [70]. Unlike SAW, in QCM sensors, the adsorption of gas is inversely proportional to the frequency shift. Quartz crystal coated with tetramethylammonium fluoride tetrahydrate (TMAF) was used for CO₂, SO₂, NH₃, and H₂S quantification in a piezoelectric sensor. Despite several advantages associated with piezoelectric sensors (including a linear response, high frequency and high transient output, and small size), these sensors suffer from high operational temperature, the small output signal (voltage), and relatively high noise [54].

1.2.3.4 Metal oxide semiconductor sensors

Metal oxide-semiconductor (MOS) sensors have widely been used in nuisance gas monitoring systems and are based on materials including tungsten trioxide (WO_3), iron (III) oxide (Fe_2O_3), tin (IV) oxide (SnO_2), indium (III) oxide (In_2O_3), barium titanate (BaTiO_3), zinc oxide (ZnO), copper (II) oxide, spinel ferrite, silver-based materials and oxides of platinum, palladium, indium, and titanium. Based on the sensing material, its thickness, and the released energy in the reaction with the gas, the conductivity of these sensors changes. They are especially desirable in H_2S detection due to their fast response, low operating temperature, and acceptable limit of detection [54]. As an example, single-crystal In_2O_3 whiskers prepared by the carbothermal method were used by Kaur et al. [71] to detect H_2S as low as 200 ppb at room temperature. The sensor was saturated at 10 ppm within 7 seconds. Thin films derived from SnO_2 crystalline sols with different mean grain sizes have also shown a great capacity in H_2S sensing [72]. Furthermore, tin oxide doped with copper oxide ($\text{Cu} - \text{SnO}_2$) films has shown great potential in the detection of pollutant gases including H_2S , SO_2 , and NO_2 at low operating temperature ($100\text{ }^\circ\text{C}$) with a large response to low concentration (10 ppm) of H_2S [73]. Finally, micromachined nanocrystalline $\text{SnO}_2 - \text{Ag}$ on a ceramic substrate (alumina) has shown an enhanced sensitivity toward H_2S as low as 1 ppm at the working temperature of $70\text{ }^\circ\text{C}$, which is much better than pure SnO_2 -based sensors [74]. Another example is tellurium thin films deposited on an alumina substrate via a thermal evaporation method which showed great sensitivity toward H_2S (0.1 ppm) at room temperature. In such a sensor, H_2S reduced the adsorbed amount of oxygen on the TeO_2 film surface, causing an increase in resistance [75]. Nanocrystalline WO_3 -based H_2S sensors are another example showing a detectability of 10 - 1200 ppm at $200\text{ }^\circ\text{C}$ [76]. Like SnO_2 -based sensors, dopants like gold, platinum, or palladium are suggested to enhance their sensitivity and operational temperature. It was found that under 1 ppm

concentration level of H₂S at 220 °C, Au - WO₃ gas sensor has a sensitivity of 23 ppm, and Pt doped WO₃ has a sensitivity of 5.5 ppm toward H₂S [77].

In all the above examples, MOS sensors are benefitting from their miniature size, ease of fabrication, acceptable LOD, low weight, and relatively low cost in mass production. However, the shortcomings associated with these sensors include high power consumption level and sensitivity toward humidity as well as cross-sensitivity, which opens up room for further optimizations and improvements [54].

1.2.3.5 MEMS sensors

Although MOS sensors are the most widely-used type of sensors for H₂S detection purposes, the necessity of having more control over the operational conditions and also optimizing the structure has led to the development of MEMS- (micro-electro-mechanical systems) based sensors to simply achieve higher sensitivities at lower temperatures [54]. To decrease the required power for heating, Gupta et al. [78] fabricated batch-processed polarization beam splitters (PBS) from thin-film micromachined silicon nitride membranes, which can be used within a MOS sensor. Ebrahimi et al. [79] used CuO-doped SnO₂ as the sensing material through a sol-gel spin coating process on porous SiO₂ substrate. The resulted MEMS-based sensor showed a LOD of 2 – 10 ppm in the surrounding environment humidity within the 25 and 150 °C temperature range, at high humidity levels (80%), which shown an infinitesimal impact on the sensor's response. Recently, a copper oxide-based MEMS gas sensor has been developed along with a temperature modulation technique for the identification of H₂S impurity in a hydrogen atmosphere. This low power gas sensor used a method of transient frequency analysis and has been shown to perform in reducing environment

and humidity level of 25% to detect hydrogen sulfide gas as low as 1 ppm within a few seconds [80].

1.2.3.6 Nano-structured sensors

Recently, there is an increasing demand to integrate nanomaterials with common gas sensing sensors to decrease the power consumption and benefit from the higher chemical reactivity to increase sensitivity (as there are more reactive sites in nanostructures due to their large surface area to volume ratio compared to bulk materials) [54]. Doped Fe_2O_3 , ZnO , and WO_3 nanoparticles were deposited on gas sensors, and H_2S was detected from 200 ppb to 1500 ppm with a LOD of 20 ppb by controlling the structural characteristics such as crystallinity and surface defects. Among the aforementioned materials, WO_3 has shown the best sensitivity at the concentration ranges of 1 to 1000 ppm within the temperature range of 40–250 °C, and the highest response was detected at the highest temperature (250 °C) [81], [82]

1.2.3.7 Sensors from organic or inorganic nanomaterials

Recently, organic and inorganic nanomaterials have been a topic of interest to be used in gas sensors because of their characteristics, including their compact size, low power consumption producing sensors with better performance in terms of sensitivity, selectivity, response time, and power consumption. As an example, CuO has become an attractive option to be integrated with conducting ionic liquid (IL) to control the conductivity and improve metal-oxides thermal and electrochemical sensing properties to obtain better selectivity toward the target compound as well as an increase in the flexibility of the deposited layer [83]. However, there are a few hindrances associated with IL, including low solubility, diffusion, and vapor pressure making it unsuitable as electrolytes and diffusion barriers in electrochemical sensors. However, organic chitosan (CS) can

be embedded with IL at different concentrations (1–9% volume/ volume (v/v)) to achieve a sensitive, low temperature and flexible H₂S sensor that maintains semiconductor properties. The resulted sensor is transparent, flexible, easy to fabricate, and detects H₂S as low as 15 ppm at 20°C with a fast response time of 14.9 ± 3.7 s [84].

1.2.4 Review of integrated devices

Manual sampling/processing is mostly used in wastewater treatment facilities to identify areas in which the target gas is of high concentrations. A manual sampling of sewerage is a health hazard due to the fact that it contains toxic and corrosive compounds. Apart from being a health hazard, it is time-consuming and labor-intensive. In essence, the extracted samples need to be analyzed once they are collected; the off-site analysis requires complex and expensive equipment such as gas chromatography (GC) or gas chromatography coupled mass spectrometer (GC-MS) detectors which eventually makes these methods not suitable and time-efficient for a dynamic wastewater system across multiple testing sites. In fact, they are bulky, mostly limited to laboratory use, and often require trained personnel to operate [85], [86].

Electronic noses (E-noses) are an alternative (to manual testing/processing for H₂S measurements) in which a feature extraction method is used for the concentration analysis [87]–[89]. However, E-nose technology uses multiple sensors sensitive to a specific gas to create a sensor array which increases the chance of independent drifts of array components, and hence frequent re-calibrations and replacements are inevitable. Colorimetric methods are also considered quantitative detection techniques for on-site applications. By arranging metal-ion-modified silica-gel powders within a glass tube, the powder color changes due to the presence of H₂S and NH₃ in the medium. As a

result, the colorimetric detector is able to yield positive/negative responses. Despite the simplicity and its in-field application, this method lacks a good limit of detection since (i) the operation range is between 100 – 3000 ppm, and (ii) the main principle behind its calibration is color and hence challenging [90].

The pulsed fluorescence technique is a commercially available method for H₂S and SO₂ measurements in air. Additionally, a fluorometric field instrument was developed by Toda et al. [91] for atmospheric H₂S measurements. It is a portable membrane-based diffusion scrubber made by polytetrafluoroethylene (PTFE) with an enhanced limit of detection (LOD) of less than 100 ppt which is operated in several field tests using a 12 V marine battery. However, this technology is inadequate for liquid sample analysis (as the humidity inhibits H₂S detection resulting in erroneous measurements [92]), has a short maintenance period, and uses fluorescein mercuric acetate (FMA) solution, which is a toxic reagent. Also, the scrubber's design affects the gas collection process. Finally, the selectivity is a challenge since it uses different separation membranes [93]–[95]. In another study [96], molybdenum sulfide/citric acid composite film was coated on a fiber grating to perform as a membrane within a core and shell design using a sol-gel and dip-coating method. By measuring the resonant wavelength shift in a long period fiber grating (LPFG) H₂S concentration will be calculated based on the induced molecular adsorption mechanism. The complexity of this type of measurement and the required equipment and inability to analyze liquid samples are a few shortcomings of this technique despite its high sensitivity and steady responses. In another study, a luminescent cellulose filter-based detector was developed which showed a high sensitivity (LOD of 2 ppb) with a reasonable response time (15 minutes). This was obtained by soaking the cellulose filter within a palladium complex which had a fluorescent ligand. Once it was exposed to H₂S gas, the ligand set free and amplified the fluorescence. Despite the high

sensitivity and fast response time, this device is sensitive to humidity, low throughput and incapable of being used for field applications [97]. The poplar branch is also used to detect H₂S by immersing the branch into Fe (NO₃)₃ solution and calcined in air to use the porous structure as a sensor. Although the technique has a great limit of detection, it suffers from high recovery and is unable to analyze liquid samples [98].

So far, all the mentioned methods are inadequate to analyze liquid samples. Vapor generation in inductively coupled plasma-optical emission spectrometry (ICP-OES) and inductively coupled plasma-atomic emission spectroscopy (ICP-AES) are two of the methods which both offer µg/L detection level for H₂S sulfide measurements in aqueous samples [99], [100]; however, some limitations are associated with these techniques including the use of chemical substances, sulfur containing compounds which form volatile compounds in an acidic environment, oxidized sulfide to non-volatile sulfur and heavy metal ions creating insoluble sulfides [99]. Liquid chromatography coupled with mass spectrometry (LC-MS) is able to analyze H₂S in aqueous solutions, but it has the same insufficiencies of GC and GC-MS [101]. Cell-based biosensors are another method for H₂S detection in liquid samples, but these sensors are restricted to the viability of the cells. As such, calibration of these sensors is difficult and they cannot be used as a reliable solution for extended periods of testing [102].

Liu et al. [6] proposed a setup capable of online communication for transmitting analysis for dissolved sulfide and methane measurement (Figure 1.4). It measures gas-phase concentration under equilibrium condition once the compounds are stripped from the liquid to gas phase and then correlates the measured concentrations to that of in the liquid phase using Henry's law. For gas-phase measurements, a commercial H₂S detector (ODASL-H₂S-2000 sensor) was used, which

measures H₂S in the headspace after being stripped. Although the limit of detection can be adjusted by changing the liquid to gas phase ratio, the system is based on the acid stripping method (to convert the dissolved sulfides to H₂S), which may not be appropriate for remote hotspot monitoring. Table 1.1 summarizes and compares available technologies reviewed in this section.



Figure 1.4 Online dissolved sulfide monitoring system and its field installation. (reprinted from [6] with permission from Elsevier)

Table 1.1 Summary of available devices for H₂S measurement.

Device	Measurement	Analytical condition	Concentration range	Limit of detection
Portable oral malodor analyzer [103]	MOS with GC	Lab-based	50 – 1000 ppb	50 ppb
E-nose system [88]	MOS	Field applications	0 – 20 ppm	-
GC with sulfur chemiluminescence detection [86]	GC along with sulfur chemiluminescence detector (SCD)	Lab-based	-	15 pg per injected sample (200 µl)
Colorimetric forensic Sensor [90]	Metal-Ion-modified Silica Powders	Field applications	100 – 3000 ppm	100 ppm
Thermo scientific 450i H ₂ S analyzer [92], [104]	Pulsed fluorescence technique	Lab-based	0.05 – 100 ppm	1.5 ppb
LPFG sensor [96]	Optical fiber grating	Lab-based	0 – 70 ppm	10.52 pm/ppm
Sensitive luminescent paper-based sensor [97]	Filter paper sensor	Lab-based	8 – 110 ppb	2 ppb
Vapor generation technique with ICP [99]	Optical emission spectrometry	Lab-based	0.06–22.0 mg/L	0.03 mg/L
Online total sulfide detector [105]	ODASL-H ₂ S-2000	Field applications	0-2000 ppm	-

1.3 Motivation

As discussed above, the current gas monitoring devices are limited according to their size, automation, online communication, liquid sample analysis, complexity, ease of use, and measuring multiple dissolved sewer gases (in particular for H_2S and NH_3). Thus, there is a need for technology to address the above challenges related to accurate and real-time measurement of multiple gases dissolved in the liquid phase of sewer lines. In this work, the microfluidic technology along with machine learning models is used to (i) increase the selectivity of the proposed sensor (being able to differentiate between H_2S and NH_3), (ii) miniaturize the detector while maintaining the rapid analysis of small samples. Identifying the “hotspots” using the proposed detector will maximize the cost-effectiveness of chemical treatments as it minimizes the amount of chemicals to inhibit nuisance gas generation and evaluates the success of ongoing treatments.

1.4 Objectives

The objective of this research is to develop a device based on a microfluidic-based detector that can be placed along pipelines for liquid-phase analysis. By detecting generation points of target gases (including noxious gases (H_2S , NH_3) dissolved in the liquid phase, the specific “hotspots” of generation can be targeted for treatment. Moreover, the developed automated setup will reduce human interaction and thereby increase the safety of wastewater treatment personnel. These goals will be achieved through the following research objectives: (1) developing a microfluidic-based gas sensor: this requires to be sensitive and selective for detection of target gases within a mixture of analytes available in the liquid waste, (2) developing an automated sample extraction and delivery system: this requires a robust system that prevents clogging in order to maintain device

functionality; this involves different stages of sample extraction, sample filtration, vaporization of a liquid sample into a gaseous state, exposing the gases to the sensor and purging the chambers, (3) developing instrumentation and control hardware to operate the detector wirelessly as well as transmitting data to an online depository, (4) developing a robust platform to integrate the detector using long-lasting materials suitable for operating based on the sewer environment conditions, (5) calibrating the setup against H₂S using standard samples; this involves numerous tests using a standard sample with a known concentration and exposing the sensor to different levels of H₂S and NH₃, and (6) conducting field tests (at Annacis Island (Delta, BC) wastewater treatment plant (AI-WWTP)) to check and optimize various tasks such as sample extraction, evaporation, and data transmission are performing automatically.

1.5 Organization of thesis

The mentioned objectives are thoroughly presented in the following chapters:

In Chapter 2, the development of the microfluidic-based detector and automated setup is explained. Chapter 3 shows the results based on pure samples in the liquid phase used for calibration, followed by Chapter 4 in which mixtures of ammonia and hydrogen sulfide are tested along with raw influent gathered during field tests. Finally, in Chapter 5, the summary of the achievements is presented along with contributions of this work and potential future work.

2 Experimental setup

2.1 Microfluidic-based detector

A highly sensitive gas sensor that is specifically designed to detect H₂S (Figure 2.1) is used for nuisance compounds detection. There are four different metallic and polymeric layers on the microfluidic channel walls to increase sensor selectivity against certain compounds such as H₂S.



Figure 2.1 The Selective microfluidic system embedded with a MOS sensor

To fabricate the microfluidic-based detector, the channel (a 3-cm long and 500- μ m high) is 3D printed using polyjet technology using VeroClear (RGD 810), and then coated with chromium, gold, and parylene C, respectively. Finally, a metal oxide semiconductor (MOS) sensor (Figaro Engineering Inc. TGS 2602) is embedded at the end of the microchannel. The sensor is capable of measuring diminutive changes in real-time, while the specialized metal and polymer layers provide enhance selectivity due to the effect of adsorption, desorption phenomena. The schematic of the

detector's microfluidic channel coated layers and diffusion of molecules are shown in Figure 2.2. The detailed fabrication process and the effect of different coatings on the detector's selectivity and sensitivity are explained in [106].

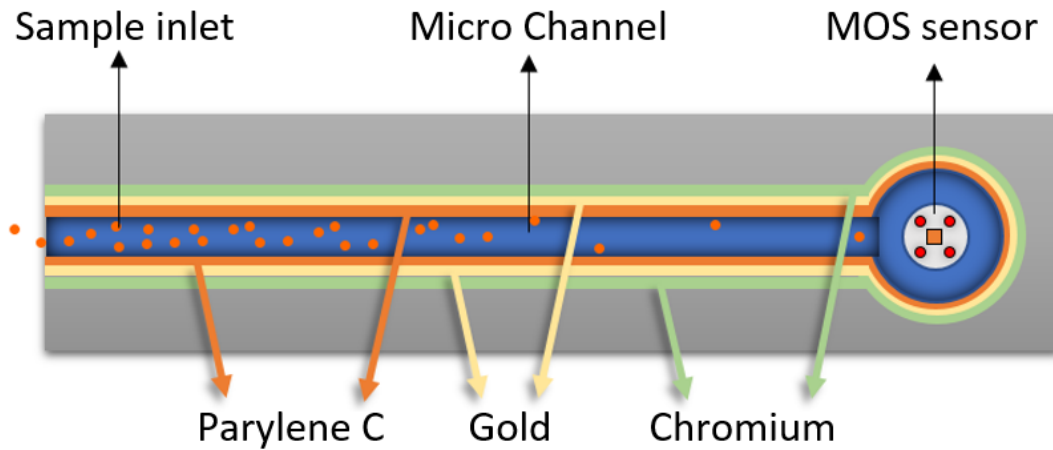


Figure 2.2 Schematic of the detector showing the channel, coatings, and the gas molecules diffusing through the channel (reprinted from [107] with permission from IEEE)

Gases and mixtures can qualitatively be analyzed using the data collected from the detector and also by considering the diffusion rate of different compounds as well as the adsorption/desorption rate inside the channel based on the available analytes and coated layers which can ultimately enable selectivity of the detector. Furthermore, a pattern recognition algorithm can be used to differentiate between target gases present in a given sample. In essence, the sensor response to different gases provides a unique set of features extracted from raw data that trains the model to recognize a particular “smell print” of target gases in the given environment. This approach not only demonstrates the presence of a gas but also computes the concentration of target gases.

2.2 Benchtop setups

During the course of this project, two main prototypes were developed for liquid H₂S analysis. In the first design (Version 1), the core sensing unit was located in a jar configuration with a mobile sensor. The second prototype (Version 2) has a different core sensing unit and the sensor arrangement is stationary. Both of these setups will be explained thoroughly within the upcoming sections.

2.2.1 Version 1

This benchtop setup is designed to extract volatile components from aqueous samples by vaporizing the sample and then exposing it to the microfluidic-based gas detector for measurements. The setup consists of a syringe pump, solenoid valves, exposure and recovery chambers, heater, and linear actuator. The detector and chamber components are sealed in a jar configuration (see Figure 2.3), and the apparatus is controlled using a microcomputer (Raspberry Pi 3 Model B+) which transmits sensor data and receives inputs from the user through a touch screen display interface. The jar configuration consists of the chambers, the heater, the linear actuator, and the detector (see Figure 2.4). The chambers and the heater have been custom designed and fabricated for specific corrosion-resistant properties. The exposure chamber is made from ultra-high-molecular-weight polyethylene coated with parylene C. The heating chamber comprises the heater and porcelain crucible for sample vaporization. The wire used in the heater is AWG 30, Omega nickel-chromium 60 resistance wire, which has the corrosion-resistant properties necessary for this application. The wire is wrapped around a porcelain crucible and coated in OMEGABOND

600 cement that is also corrosion-resistant. Figure 2.5 shows the inside view of the jar configuration that contains the MOS sensor and the heating chamber.

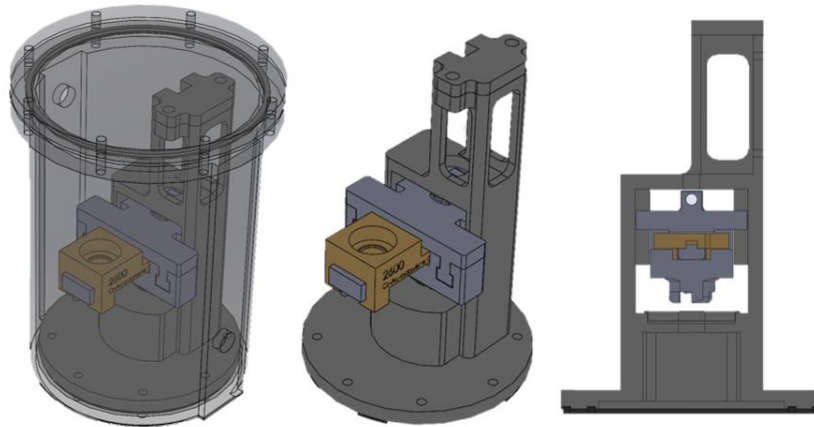


Figure 2.3 Sensor's housing

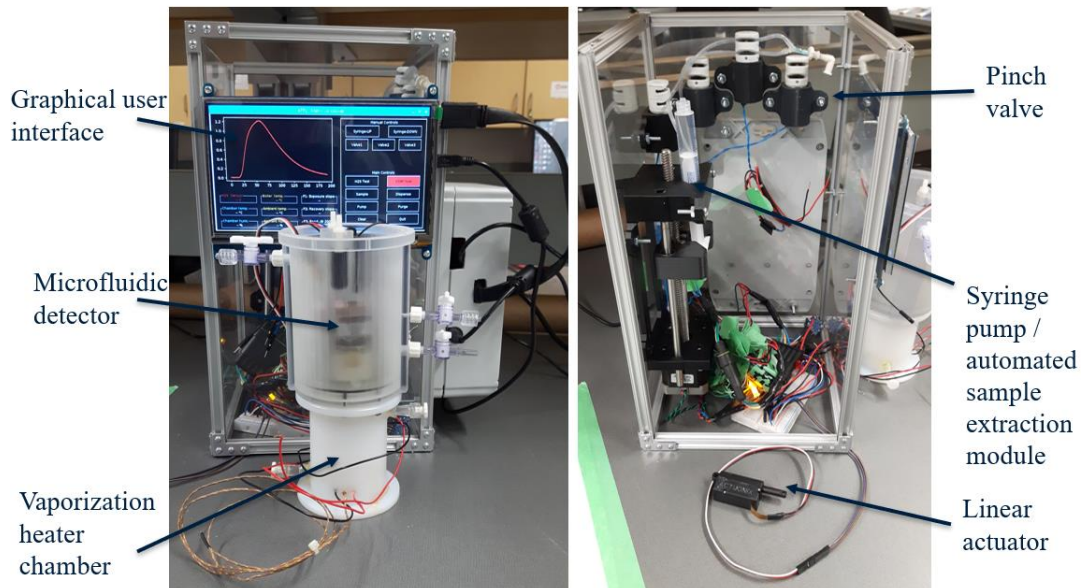


Figure 2.4 Version 1 prototype device: (a) major components include a rechargeable power source, touch-controlled graphical user interface, sample vaporization, and gas sensing modules; (b) key internal components for automated sample extraction.

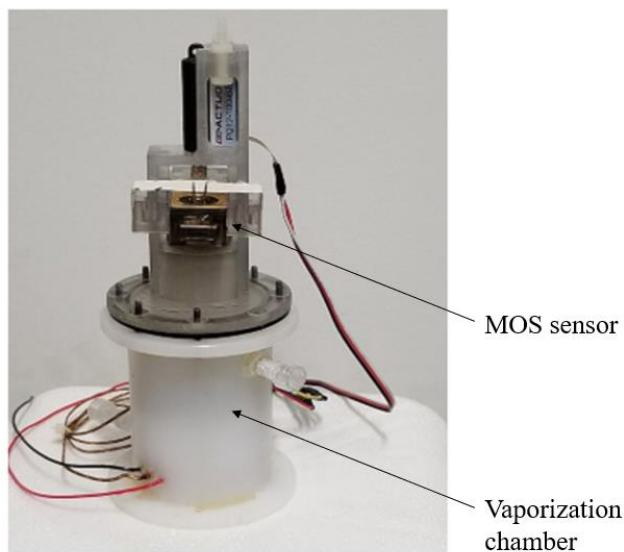


Figure 2.5 The jar configuration, including the microfluidic-based detector and the vaporization chamber

The testing procedure of the setup consists of 4 steps: Sample extraction, vaporization, exposure, and recovery.

- 1. Sample extraction:* A custom-made syringe pump powered by a stepper motor along with a series of solenoid valves delivers a 1-mL sample to the vaporization chamber free of air bubbles.
- 2. Vaporization:* Once the sample has reached the vaporization chamber, the heater is activated and remains on for 240 seconds to ensure complete vaporization of the sample. There is no data recorded during this time.
- 3. Exposure of microfluidic-based detector to target analytes:* Once the sample is completely vaporized, the detector is exposed to the sample vapor, and data logging begins. This portion of the data collection continues for 42 seconds.

4. *Microfluidic-based detector recovery*: After the detector is exposed to the sample, it is exposed to fresh air for 260 seconds, at which point the data collection stops and the test cycle is complete.

2.2.2 Version 2

The major problems of Version 1 were the complexity of the sample extraction method, lengthy overall test time, and bulkiness of the setup. Moreover, collected data from this version revealed noises due to the detector's movement during the exposure and recovery time. As a result, the Version 2 prototype was conceptualized (see Figure 2.6 and Figure 2.7 showing outside and inside, respectively). In the following subsections, the insufficiencies and developments of each component from Version 1 to 2 are explained in detail.



Figure 2.6 Version 2 (Outside configuration)

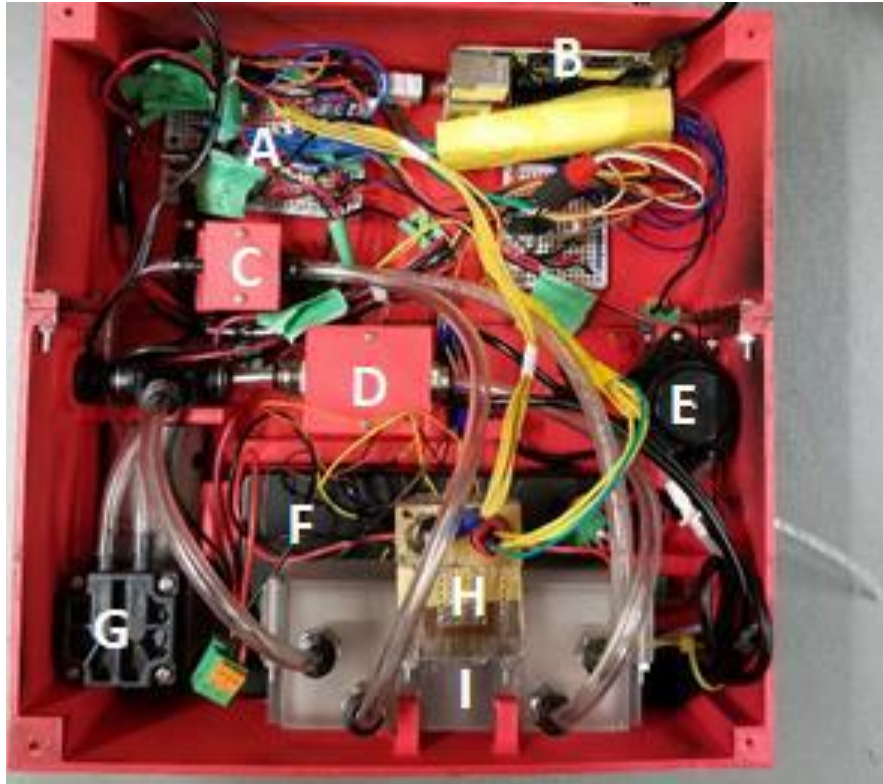


Figure 2.7 Version 2 (inside configuration): A - Protoboard, B - Raspberry Pi, C, and D - Purging valves, E - Peristaltic pump, F - Battery, G - Purging pump, H - Microfluidic-based detector, I - Exposure and recovery valve.

2.2.2.1 Sensor arrangement

In addition to the single-channel microfluidic-based detector, the new prototype is capable of installing different types of sensors with different channel sizes. Different sensors, including electrochemical sensors (EC) and other MOS sensors can be mounted on the core sensing unit, and the sensitivity and selectivity of the current microfluidic-based detector, which uses an H₂S MOS sensor (Figaro Engineering Inc. TGS 2602) can be compared with commercial electrochemical sensor (H₂S-MD- 700 MGK SENSOR Co., Ltd.) or an NH₃ sensor (Figaro Engineering Inc. TGS 826).

Comparing the electrochemical sensor to the H₂S MOS (Figaro Engineering Inc. TGS 2602), the electrochemical sensor requires additional equipment (VersaSTAT 4) to read the received signal, although it showed higher sensitivity during experiments. However, the MOS sensor doesn't require any additional equipment to read the signal, and it uses an onboard chip (16Bit I2C ADC+PGA) to collect data. To benefit from the advantages of an electrochemical sensor, a potentiostatic circuit was designed and used on the portable setup, but the collected data were not as sensitive as those collected by VersaSTAT 4 (Figure 2.8). Also, the electrochemical sensor requires a more advanced purging system in order not to detect anything within the vicinity other than the extracted sample, and the reason why it requires advanced purging is because of being highly sensitive to volatile compounds meanwhile, in the MOS sensor a basic air purging will bring down the sensor to the regular working condition (further explained in Objectives 4-5 Next Steps).

Since primary effluent and influent samples both have a considerable amount of ammonia, an ammonia sensor (Figaro Engineering Inc. TGS 826) was embedded within a dual-channel microfluidic-based detector. The optimally designed microchannel was coated with layers of Chromium, Gold, and Parylene C to maintain a similar adsorption-desorption phenomenon on channel walls (Figure 2.9). The tests showed that the exposed concentration of ammonia is less than the lower detection range of the ammonia sensor, and it was not capable of picking up any signal from primary effluent or influent samples.

Considering all of the above options, using a hydrogen sulfide MOS sensor embedded with the particular geometry and coating of the channel provides an innovative way to selectively detect

gas species via their diffusion patterns before contacting the MOS sensor, and TGS 2602 was chosen as the sensor for the detector.

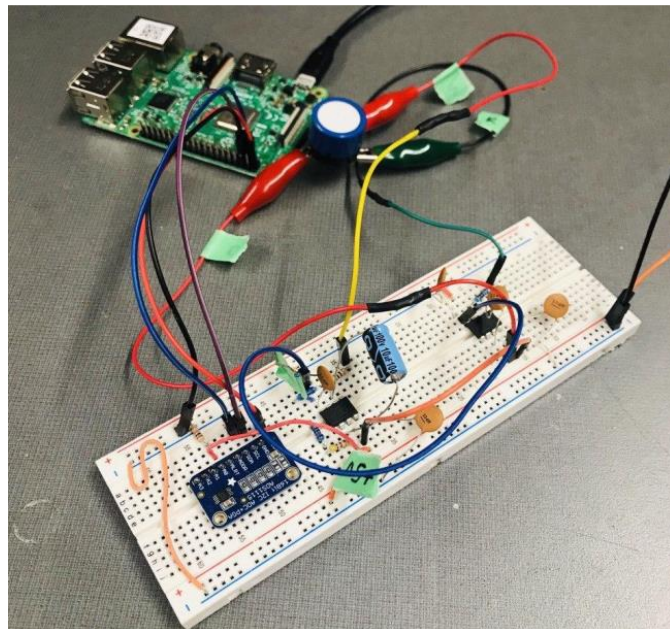


Figure 2.8 The designed potentiostatic circuit to replace the VersaSTAT 4.

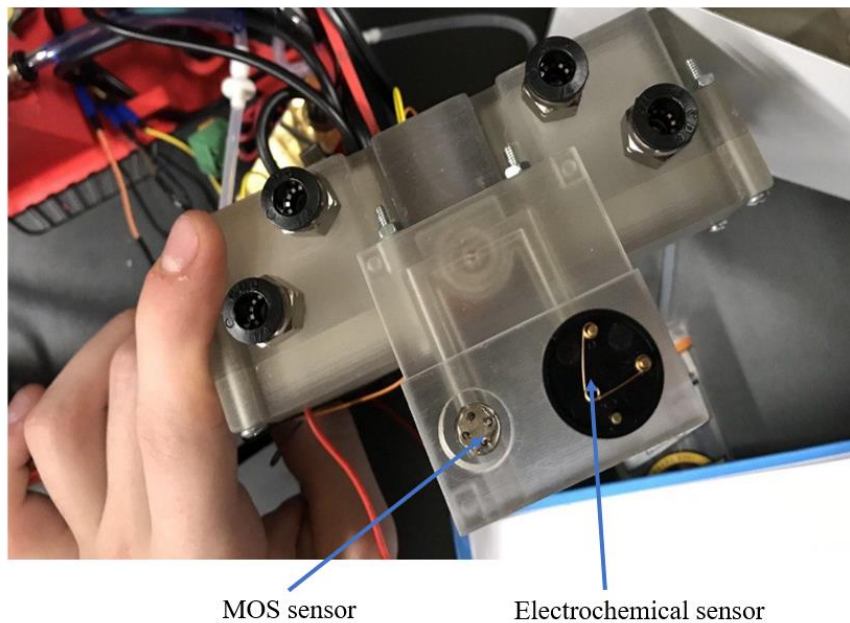


Figure 2.9 MOS and electrochemical sensor arrangement on an uncoated 3D printed dual channel detector.

2.2.2.2 Vaporization chamber and heater

The jar configuration in Version 1 has some inefficiencies in vaporization and exposure that required modifications and improvements on the core sensing unit. In the first version of the setup, a valve was designed with magnets and an Actuonix PQ12 actuator, controlled by a microcomputer (Raspberry Pi 3 Model B+), which pushed the device into a sealed position, exposing the gas sensor to the sample and subsequently pulled the device back to the recovery position. Using the sensor in a non-stationary position and exposing the magnets to H₂S caused a significant level of corrosion which was against the reliability and could potentially decrease the life cycle of the setup (Figure 2.10). Figure 2.11 shows the positioning of magnets in the sealing or exposing mechanism.



Figure 2.10 Corroded magnet in Version 1.

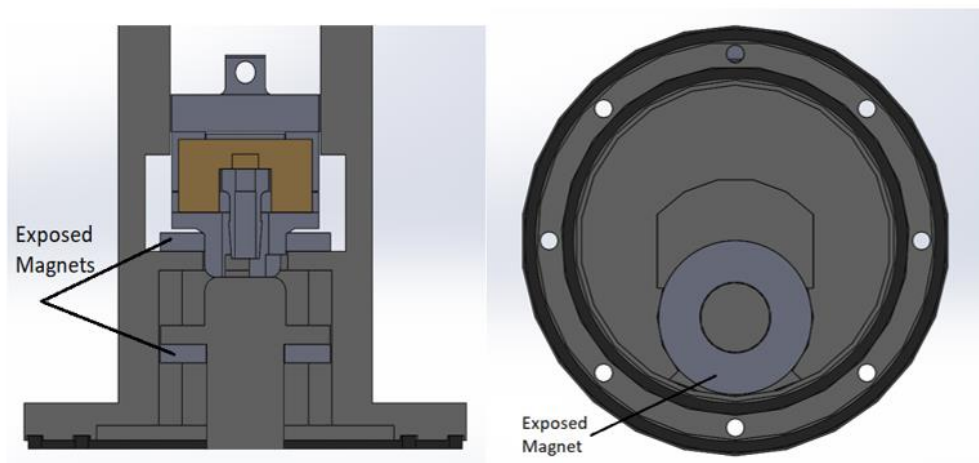


Figure 2.11 Magnets inside the jar configuration in Version 1.

Also, a compact and chemically resistant sample heater was developed through iterative stages to vaporize an aqueous sample following the extraction process. The final iteration of the heater design involved the use of the Omega nickel-chromium 60 resistance heating wire of 30 AWG wrapped in a spiral pattern around a Chemglass porcelain crucible with high-temperature OMEGABOND 600 cement (Figure 2.12). In this heater, 1ml of liquid samples were fully evaporated in 3 minutes.

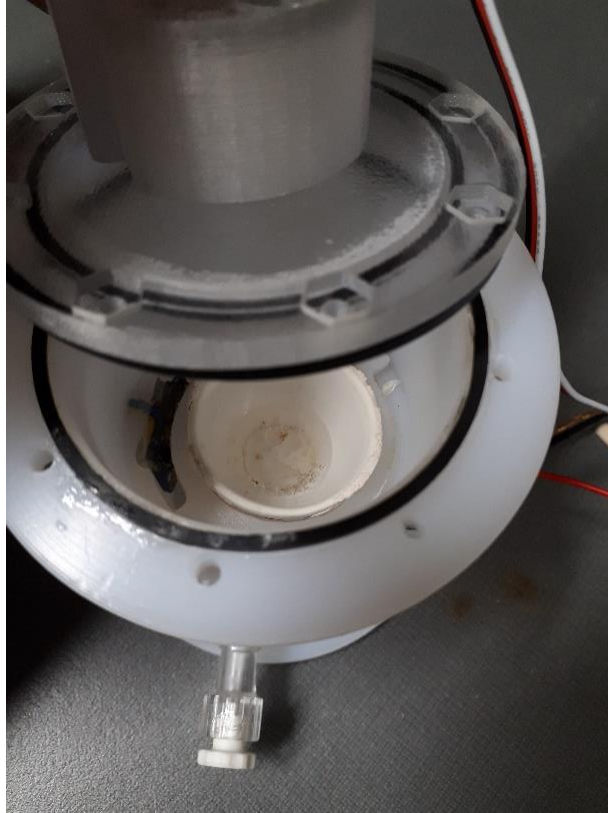


Figure 2.12 The porcelain crucible inside the vaporization chamber.

As mentioned before, the major objectives of Version 2 were to simplify the sample delivery system, reduce the vaporization time, and provide a more compact and practical form factor. Thus, a smaller chamber was designed and 3D printed in which a sample chamber and a fresh air chamber were separated by a slider that could easily switch between exposure and recovery stages. Figure 2.13 shows the section view of the 3D printed compact chamber. As it can be seen, the slider is controlled by a servo (Adafruit micro servo - high powered, high torque metal gear) that enables the slider's movement during recovery or exposure. To vaporize liquid samples, the sample is pumped directly onto the heating element through the top of the sample chamber. After vaporization, the sealing slider rotates to expose the sensor to the vaporized sample (left image of

Figure 2.13). After sample exposure, the sealing slider rotates back to seal the sensor from the sample while allowing clean air to recover the sensor (right image of Figure 2.13).

O – rings were used for sealing purposes, and for better sealing and reducing friction a lubricant was applied on the contact surface of the slider’s path. This design allowed us to use any sensor on top of the vaporization chamber without any size restrictions. Moreover, having the sensor in a stationary position led to collect data with less noise.

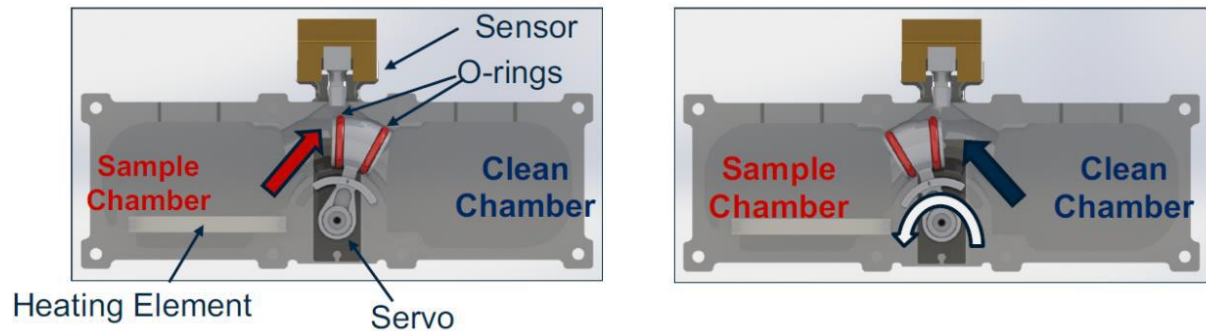


Figure 2.13 Exposure and recovery chambers section view.

Furthermore, a stepper motor driven system (NMB technologies corporation PG20L-D20-HHC0 step motor geared bipolar 10V) was also designed to be compared with a servo motor to choose the best option to minimize noises in collected data during slider’s movement (Figure 2.14). Comparing two different actuators for rotating the slider, the servo motor moved quickly and had higher torque. This torque allowed the chamber to be sealed better. The stepper motor allowed for better speed control but lacked the torque of the servo motor, and as a result, the sealing was worse. After testing, the servo motor produced smoother and more consistent results.

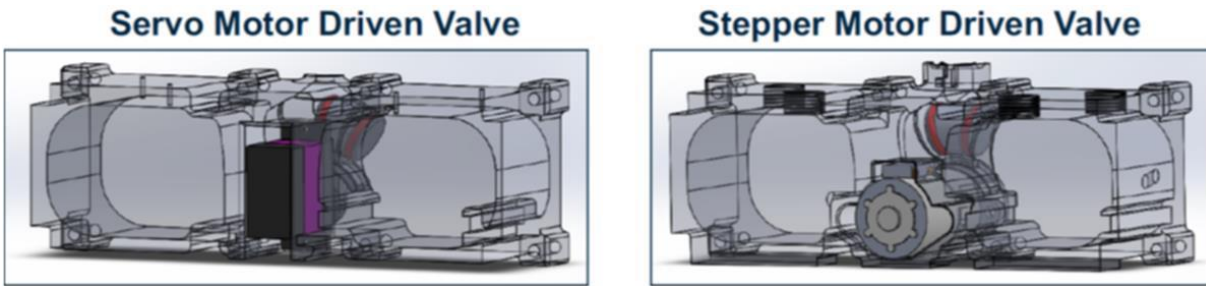


Figure 2.14 Exposure and recovery valve motor comparison.

To reduce the vaporization time, a new heating element with a greater surface area was used. A 3D printed container was used as an attachment on top of the heater to avoid any sample overflow (Figure 2.15). This heater decreased the evaporation time of 1 ml liquid to more than 50 percent, which allowed the system to evaporate 1ml of liquid sample in 80 seconds.

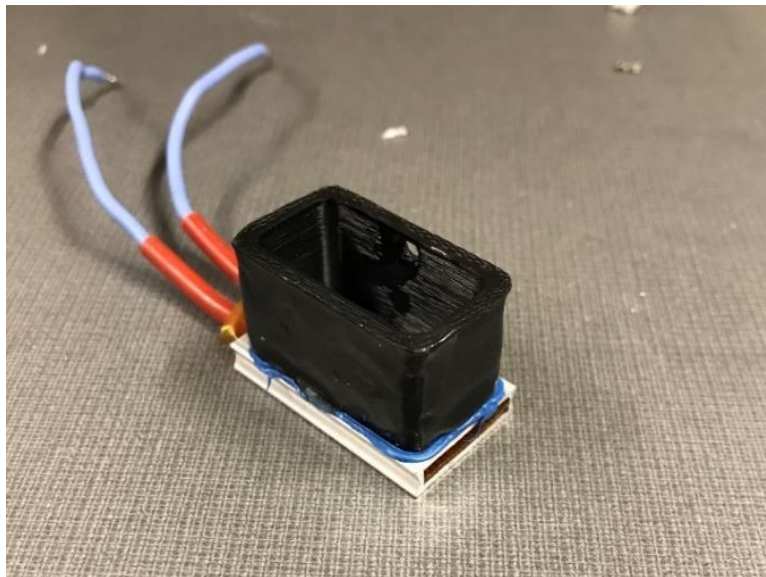


Figure 2.15 The new heating element with the 3D printed container.

In summary, this innovative exposure and recovery valve design that was used in Version 2 allowed for the sensor to be stationary for better data consistency. In the meantime, it eliminated the use of magnets that were susceptible to corrosion, and the new valve design with a modular

twist-and-lock mechanism easily enabled attaching and detaching of different sensor configurations. Figure 2.16 shows the final 3D printed vaporization/recovery chamber used in Version 2.

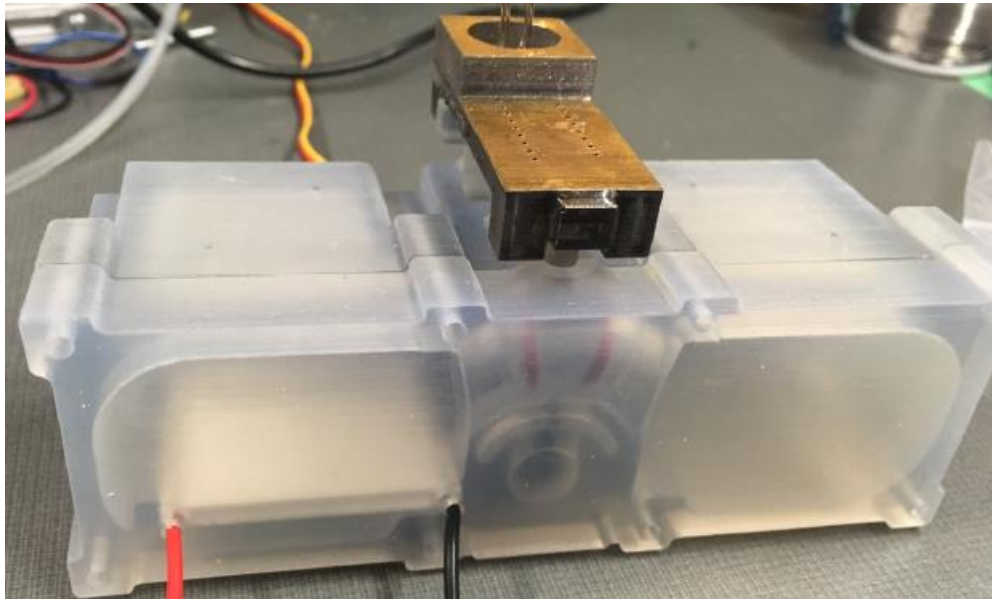


Figure 2.16 The final design of vaporization chamber and heater.

2.2.2.3 Sample delivery system

At this stage, a platform is required to transport a discrete proportion of the collected sample to a vaporization chamber. The previous stepper motor-driven syringe pump used for sample extraction in Version 1 was replaced with a peristaltic pump (Adafruit peristaltic liquid pump with silicone tubing) (Figure 2.17). This pump both extracted the sample quickly and accurately but also eliminated the need for all four pinch valves. Version 1 required a tedious process to ensure that no sample was trapped between the pinch valves. With the new pump, the lines could be cleared by running the pump in reverse. This method could also be used with or without sample filtration.

The sample extraction upgrade worked towards all three major objectives and eased sample extraction.



Figure 2.17 Adafruit peristaltic liquid pump with silicone tubing.

2.2.2.4 Purging system and filtration

To use influent or effluent samples, filtration is required to keep the sample chamber clean and ensure the sensing unit is not in contact with microorganisms or debris that can interact with the sample and bias the sensor reading or create nuisance compounds (acid generation via oxidization of H_2S to H_2SO_4). Collected samples should go through two stages of filtration: (1) a coarse filter will remove large particulate matter (green filter in Figure 2.18) (0.8/0.2 μm Supor Membrane® PALL life sciences) and (2) a filter with a pore size of 0.1 μm (white filter in Figure 2.18) (PALL – AP4523) to prevent the entry of smaller particles.



Figure 2.18 Filter arrangement.

Once data collection is completed, sample and clean chambers would undergo a purging process using an air compressor at 30 psi or a gas pump and a series of solenoid valves to control airflow. The duration of purging was set to 150 seconds for each chamber after extensive tests to optimize the purging time. Figure 2.19 shows how fresh air enters and exits each chamber controlled by a series of solenoid valves.

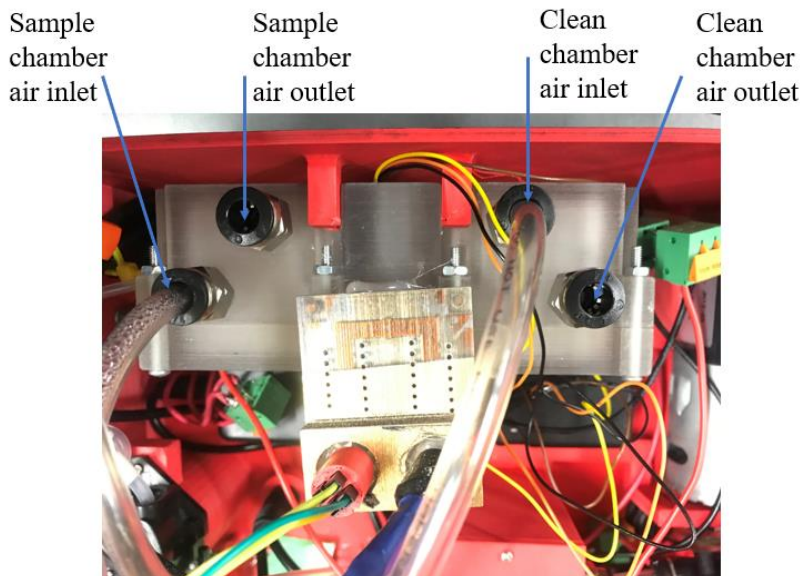


Figure 2.19 Purging inlets and outlets.

2.2.2.5 Testing procedure and data capture

A testing procedure is established for the setup, which consists of 5 steps: Sample extraction, vaporization, exposure, recovery, and purging.

(a) *Sample extraction*: A pump delivers a 1 mL sample to the vaporization chamber free of air bubbles.

(b) *Vaporization*: once the sample has reached the vaporization chamber, the heater is activated and remains on for 90 seconds to ensure complete vaporization of the sample. There is no data recorded during this time.

(c) *Sensor exposure*: once the sample is completely vaporized, the sensor is exposed to the sample vapor, and data logging begins. This portion of the data collection continues for 42 seconds.

(d) *sensor recovery*: After the sensor is exposed to the sample, the sensor is exposed to fresh air for 158 seconds.

(e) *Purging*: right after the recovery stage, the data collection stops, purging will be started. Each chamber is purged for 150 seconds to remove any sample residue.

The entire process is operated by a Raspberry Pi microcomputer. The time-series sensor response data is stored on the Raspberry Pi and transmitted to a cloud repository. To control the system, a software has been developed in which every stage can be monitored with a laptop or even on a cellphone. Just like the graphical user interface (GUI) of Version 1 (Figure 2.20), the updated interface in Version 2 is also able to show the test result and enables the option of either starting a

test or terminating the whole process (Figure 2.21). It also includes manual control over the valves, the pump, heater, slider, and it can show the most recent sensor's signal. Sample delivery, heater efficiency, and purging can be diagnosed by clicking on a button available in the manual controls window (Figure 2.22). For long-run tests, there is another interface that shows the number of completed tests and a progress bar to see the remained process (Figure 2.23).

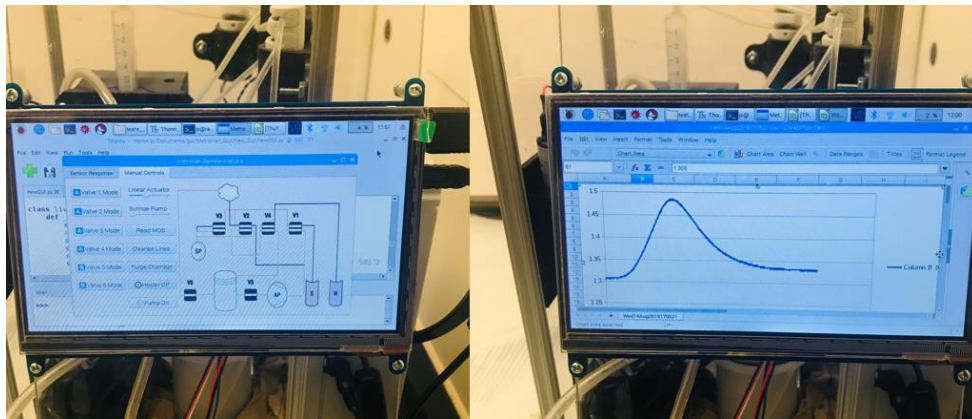


Figure 2.20 The graphical user interface in Version 1.

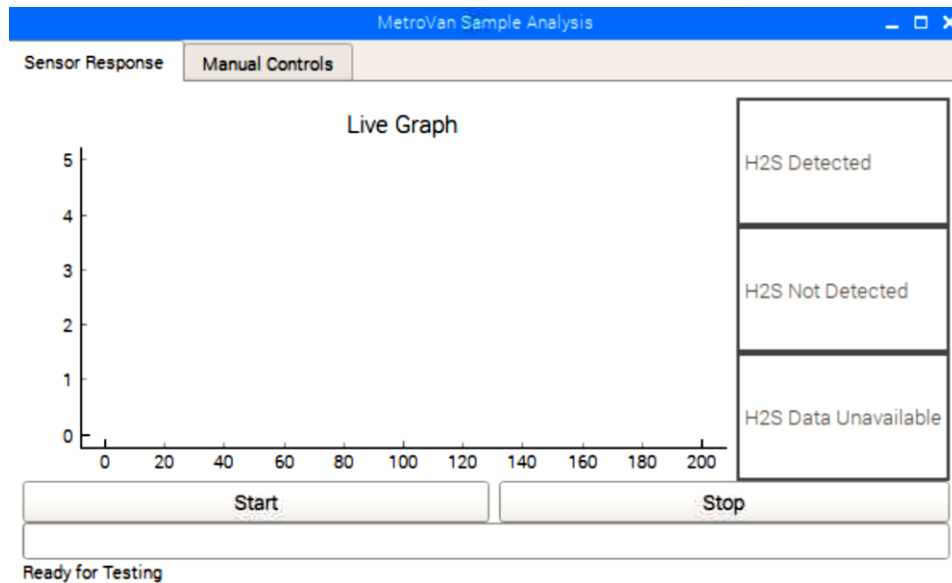


Figure 2.21 Main window of the graphical user interface.

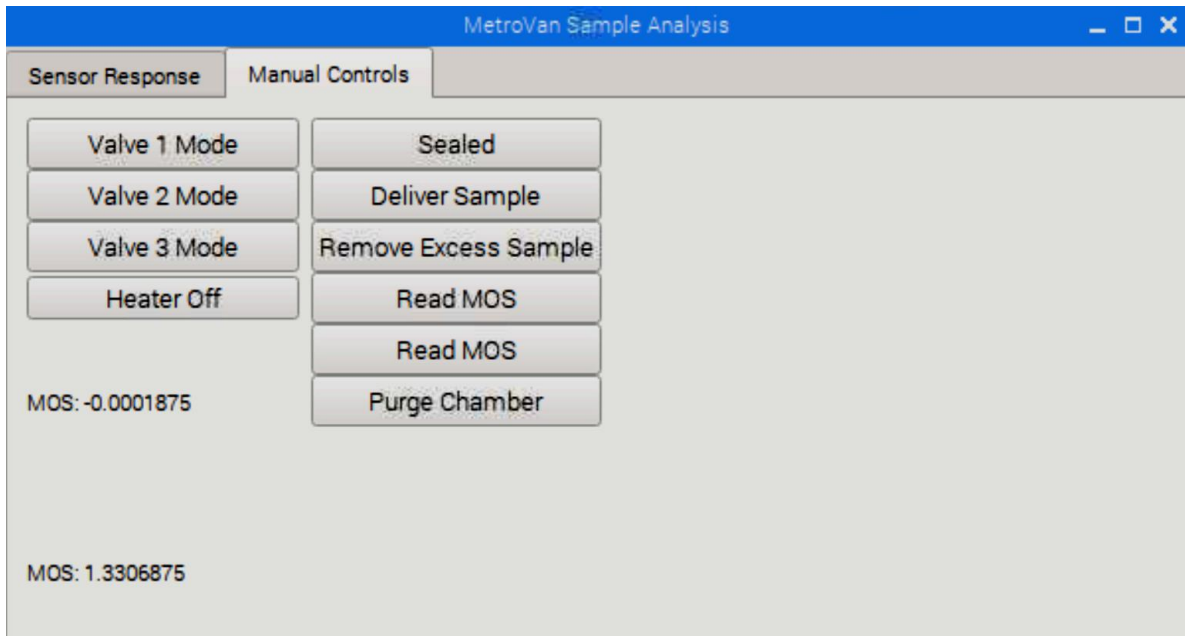


Figure 2.22 Manual controls of the interface.

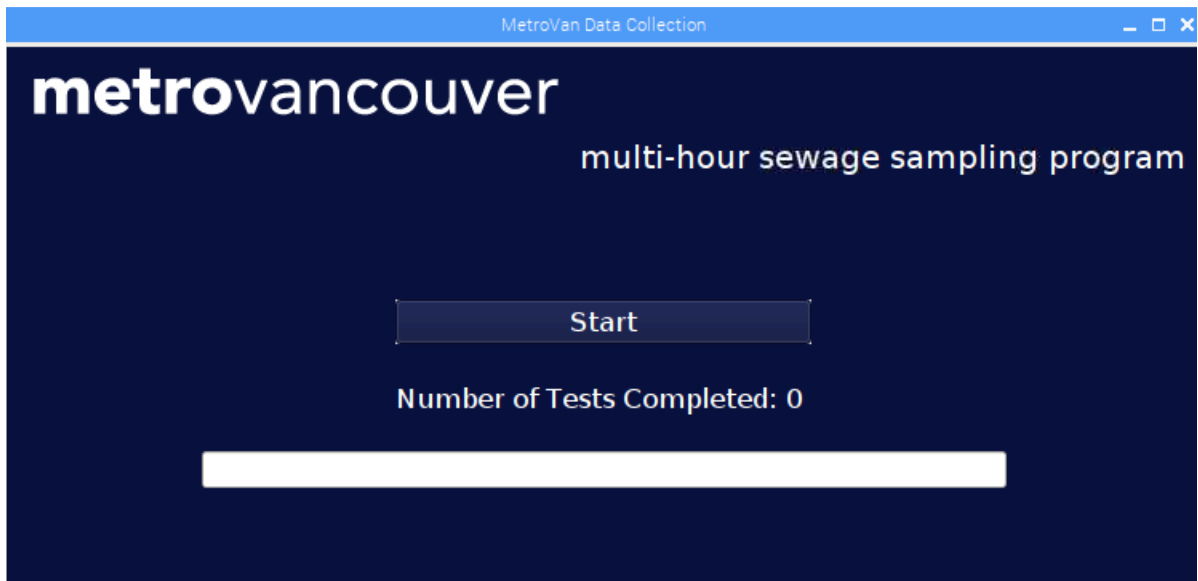


Figure 2.23 Long-run test's user interface.

3 Results of individual gases

3.1 Consistency and longevity tests

To properly measure the presence and concentration of H₂S in any sample, first, we need to make sure that the sensor is collecting reproducible and reliable data. To examine collected data, a dual-channel detector was designed and coated with Cr, Au, and Parylene C. During a 4-hour continuous test (23 tests in total), all the experimental parameters (including exposure method, sample concentration, recovery, and purging time) were kept the same to evaluate the behavior of two similar sensors (Figaro Engineering Inc. TGS 2602). Figure 3.1 shows the response of two H₂S sensors, conditioned at the same time, of the same batch received from the manufacturer and being exposed to a constant concentration of H₂S dissolved in water. The first three tests belong to the beginning of the testing cycle, and the last curve shows the responses for the last test within the 4 hours.

The results confirm that the collected signal is similar, as long as all the sensors are conditioned and exposed in the same manner. The only difference is in the baseline (representing the initial voltage of the sensor), which can be removed during the data analysis part. Also, the comparison of the responses of each individual sensor over the 4-hour test proves the great longevity of this sensor.

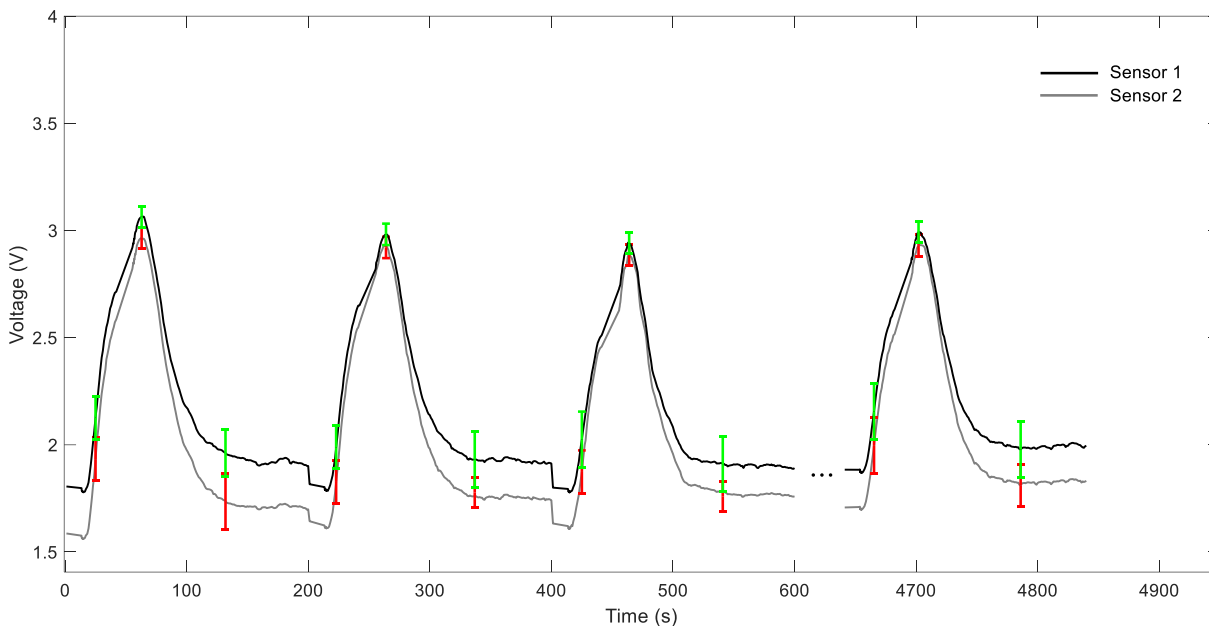


Figure 3.1 The response of two TGS 2602 sensors being exposed to a similar sample. The first three curves are for the first three tests and the last curve shows the 23rd test (last test).

3.2 Characterizing tests

The lowest detectable concentration using the sensor within the setup was determined by a wide range of aqueous-based H₂S samples. The results show that the maximum voltage increases when the sensor is exposed to an H₂S solution and decreases when exposed to fresh air (the recovery stage). As it can be seen in Figure 3.2, the maximum voltage and sample concentration are correlated. A diminutive delay also exists in detector response once it is exposed to fresh air, during which the voltage drops gradually due to the adsorption and desorption phenomenon.

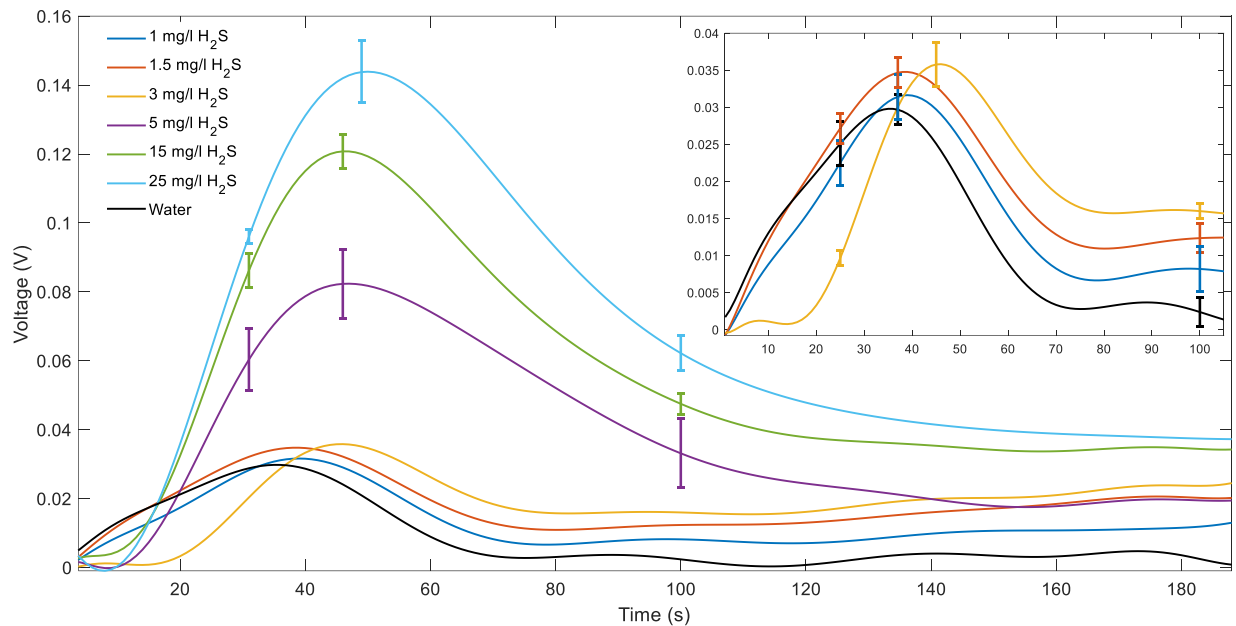


Figure 3.2 Detector response to H₂S dissolved in water. The inset shows responses to water and low H₂S concentrations.

Humidity also plays an important role when a gas sensor is exposed to a liquid sample. To distinguish the impact of humidity, especially in low concentrations, the detector responses to low H₂S concentrations and water are compared in Figure 3.2 (see the inset). The results show that the detector responses for water, 1 mg/l, and 1.5 mg/l H₂S samples are very close, especially in the exposure stage and considering the errors. The differences between the water and H₂S samples are more pronounced at the 3 mg/l concentration. Thus, it is safe to conclude that considering the effect of humidity in using a liquid sample, the lowest concentration that can reliably be detected by this detector is 3 mg/l of H₂S in water.

3.3 Ammonia results

Along with measuring hydrogen sulfide, ammonia is also needed to be quantified as it is the other major compound in sewerage. Similar to H₂S experiments, the detector was tested in different concentrations of ammonia based on the ammonia level in real sewage samples. Figure 3.3 shows the detector responses to the ammonia sample as compared to those of hydrogen sulfide. The results depict that the voltage decreases as the ammonia concentration increases. Also, for the same concentration, the detector response shape to ammonia is different than that of hydrogen sulfide.

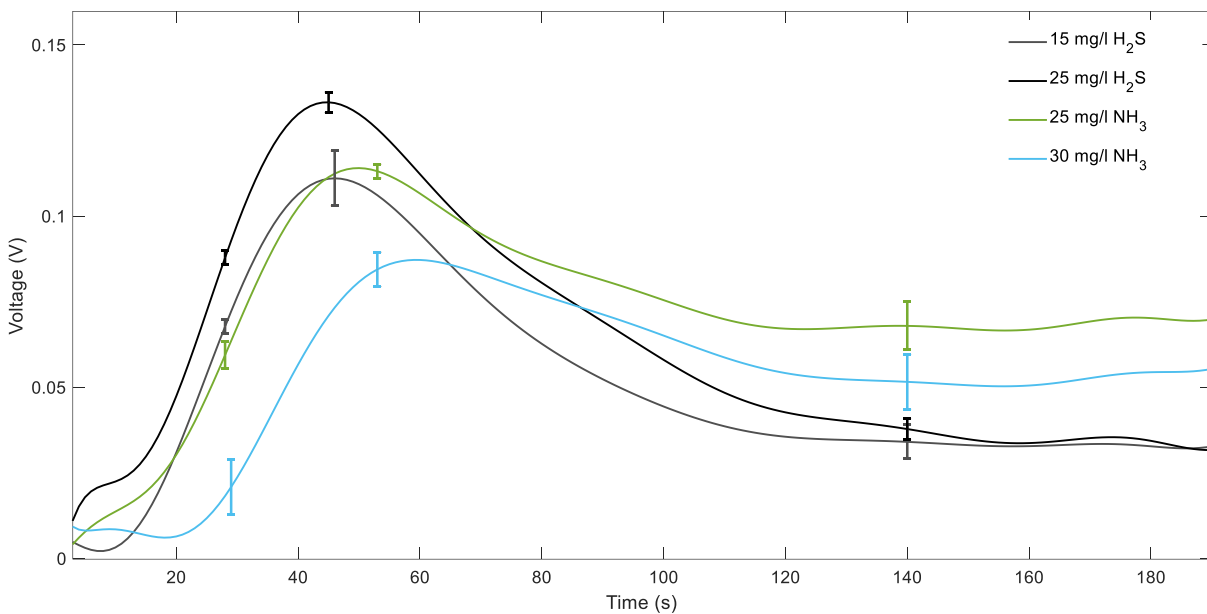


Figure 3.3 Comparing detector response to ammonia and hydrogen sulfide present individually in aqueous samples

3.3.1 Classification and regression

By obtaining the response of the detector it is clear that numerous features differ between the response of H₂S and NH₃. To differentiate between NH₃ and H₂S, a machine learning model was

trained and used as a tool to extract features from collected data to identify the unique characteristic of H₂S and NH₃ signals. The model is able to output the presence of H₂S and NH₃ in the sample.

Using the collected data from a wide range of H₂S concentrations in the liquid phase, a database for a regression model was created. The regression model uses the overall shape of the responses and gathers numerous features from data points to output the availability and the concentration of hydrogen sulfide. For the analysis of the variation, a machine learning model was employed to both qualitatively and quantitatively assess the sensor response. For the pure sample model training, 68 samples were used in total. Of the 68 samples, 56 samples contained H₂S, 9 samples contained NH₃, and 3 were only water (as a negative control). This dataset was split into a testing and training dataset, with the testing dataset size of 40% of the overall data. The first step in analyzing the data was to reduce the complexity of the data while maintaining the features and relationships. The common techniques used for dimensionality reduction include Principle Component Analysis (PCA), Independent Component Analysis (ICA), and Linear Discriminant Analysis (LDA). ICA is normally used for the separation of overlapping signals, which makes it an optimal choice for this application, as it helps separate the wanted signal from the noise.

The second step is model selection for classification. To ensure the best selection, numerous models were tested. This included Multi-Layer Perceptrons (MLP), Decision Trees (DT), K-Nearest-Neighbours (KNN), Ensemble Classifiers like AdaBoost, and Support Vector Machines (SVM). Each model was trained with 60% of the ICA-transformed dataset and tested against the remaining sets. From the various tests, the combination of ICA and SVM proved to be the most accurate. Overall, 96% recall in classifying H₂S and 100% recall in classifying NH₃ was achieved using the combination of ICA and SVM.

Finally, a separate model selection step was used for regression. Similar to classification, numerous models were evaluated for their effectiveness. This includes MLP, SVM, KNN, and DT, specifically Extra-Trees Decision Trees. Each of these models was trained with the same dataset given to the classifier, with targets as the concentration information. The output of the regressor was multi-output, therefore provided with information related to H₂S and NH₃. The extra-trees model proved to have the highest precision (84.6%) and was therefore chosen.

3.4 Discussion

The results from using plain water revealed that humidity plays an important role during each experiment. A study has been conducted to use a diffusion-based membrane to mitigate the effect of humidity during gas detection by a MOS sensor [108]. Here, the humidity level is almost consistent in all the experiments regardless of the sample being tested (both H₂S or NH₃ are in the aqueous phase and being tested at a relatively similar concentration dissolved in water). Once the analyte is evaporated, the sensor was exposed and thereby recovered right after exposure. Optimized purging time was conducted long enough to be sure the surface of each chamber is dry, and there is no residue left. Also, all data are compared with each other – not against gas samples. Thus, the humidity effect is the same in obtaining different H₂S levels.

4 Mixture results

4.1 H₂S and NH₃ mixture

To replicate the raw influent, its main components (H₂S and NH₃), which the sensor is responsive to, were mixed, and the solution was exposed to the sensor to assess the signal. Subsequently, samples consisting of NH₃ and H₂S were properly mixed at 4 different combinations meeting the lower and higher concentrations of ammonia in influent.

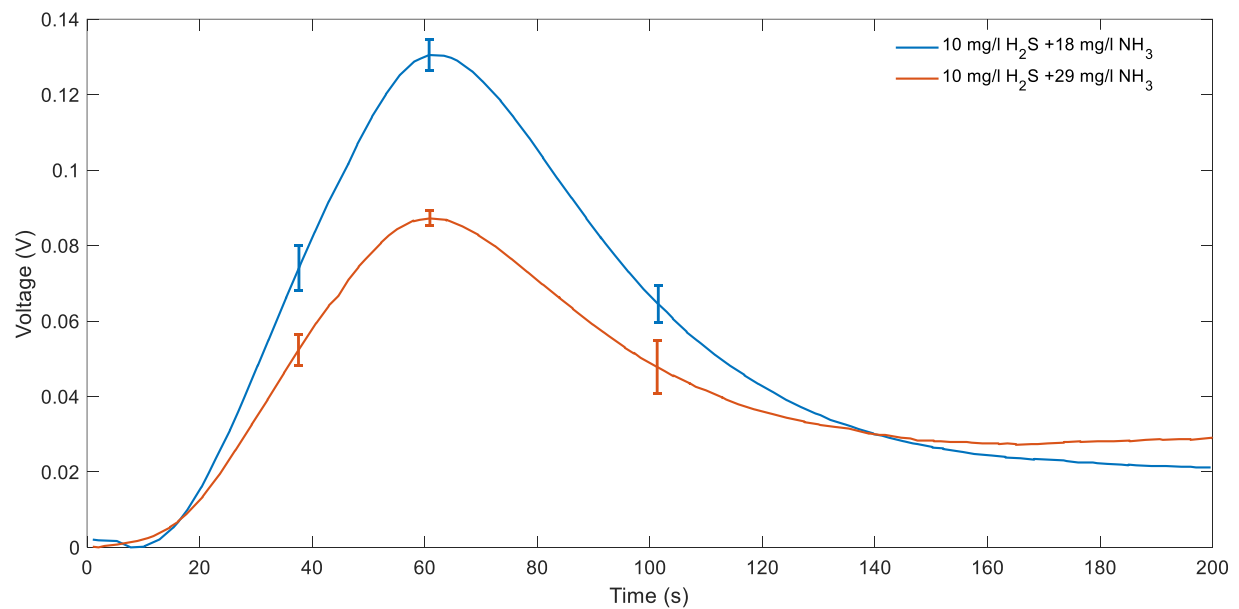


Figure 4.1 Increasing NH₃ concentration from 18 to 29 mg/l at a constant level of H₂S at 10 mg/l.

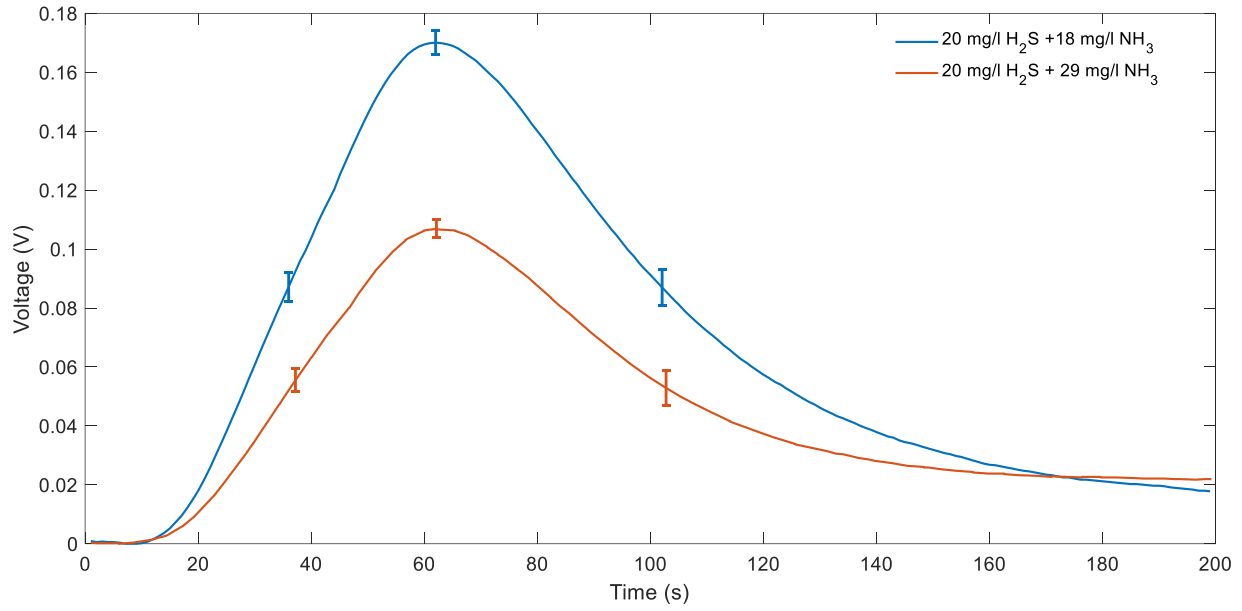


Figure 4.2 Increasing NH₃ concentration from 18 to 29 mg/l at a constant level of H₂S at 20 mg/l.

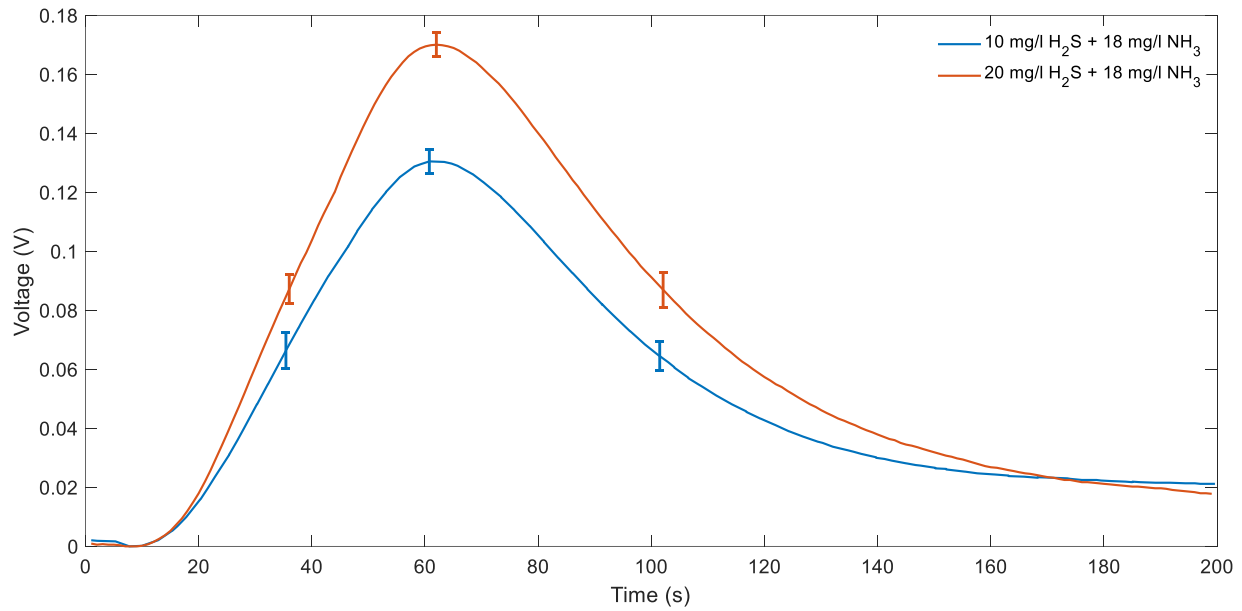


Figure 4.3 Increasing H₂S concentration from 10 to 20 mg/l at a constant level of NH₃ at 18 mg/l.

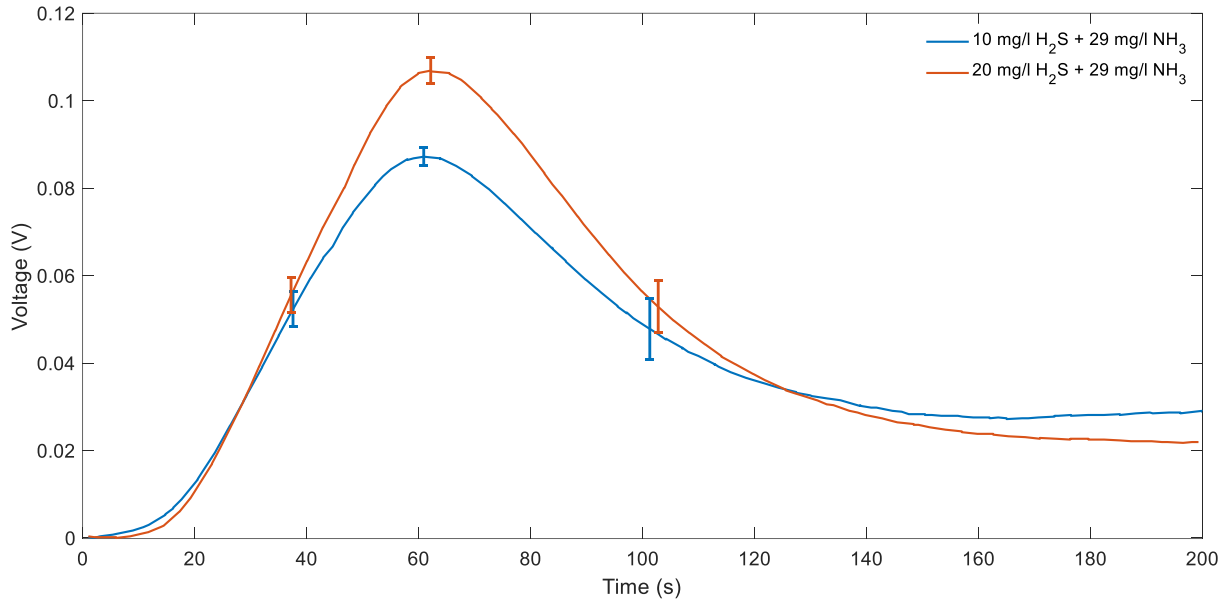


Figure 4.4 Increasing H₂S concentration from 10 to 20 mg/l at a constant level of NH₃ at 29 mg/l.

Figure 4.1 and Figure 4.2 show that by increasing ammonia in the sample at a constant level of H₂S, the magnitude of the response decreases. Moreover, Figure 4.3 and Figure 4.4 show at a constant concentration of ammonia, if H₂S increases, the magnitude of the response increases. These results are in agreement with the trends acquired from tests conducted with pure H₂S and NH₃ samples.

4.2 Classification and regression

Similar to the steps taken with the pure sample data analysis, the data collected for H₂S and NH₃ mixture was included in the dataset, and the model was trained. Keeping the models developed for the pure sample dataset, the models were updated with the additional data. The new dataset now contains the previous 68 data points from the pure samples and an additional 32 data points of various ratios of mixtures of H₂S and NH₃. The new models were trained following similar

parameters as before. The classification model returned a recall value of 96.88%, with H₂S classification 97% and NH₃ classification of 96%. A regression model was trained on the same data, resulting in a precision of 88.77% in determining the concentration.

4.3 Field test

After the device was tested for the long run showing continuous, reliable data collection, it was installed to continuously measure H₂S in the sewer pipe. Figure 4.5 shows the detector installed during the field test. Detector's responses to raw influent are plotted in Figure 4.6. These results were once again used in the previously mentioned machine learning models, and the output showed 21.85 mg/l H₂S and 9.4 mg/l NH₃ in the tested sample during the field test.

Field test results tend to have a slightly higher magnitude compared to the mixture of H₂S and NH₃ previously tested. This could be due to the fact that there are more ongoing complex interactions among all the available analytes compared to only H₂S and NH₃ interactions in the replicated samples. The other reason is related to the sewage flow condition. Since the liquid inside the swage pipe subsidiary (shown in Figure 4.5) is stationary, bacterial activity increases (as time goes by), which leads to more H₂S generation that eventually affects the magnitude of the overall response.

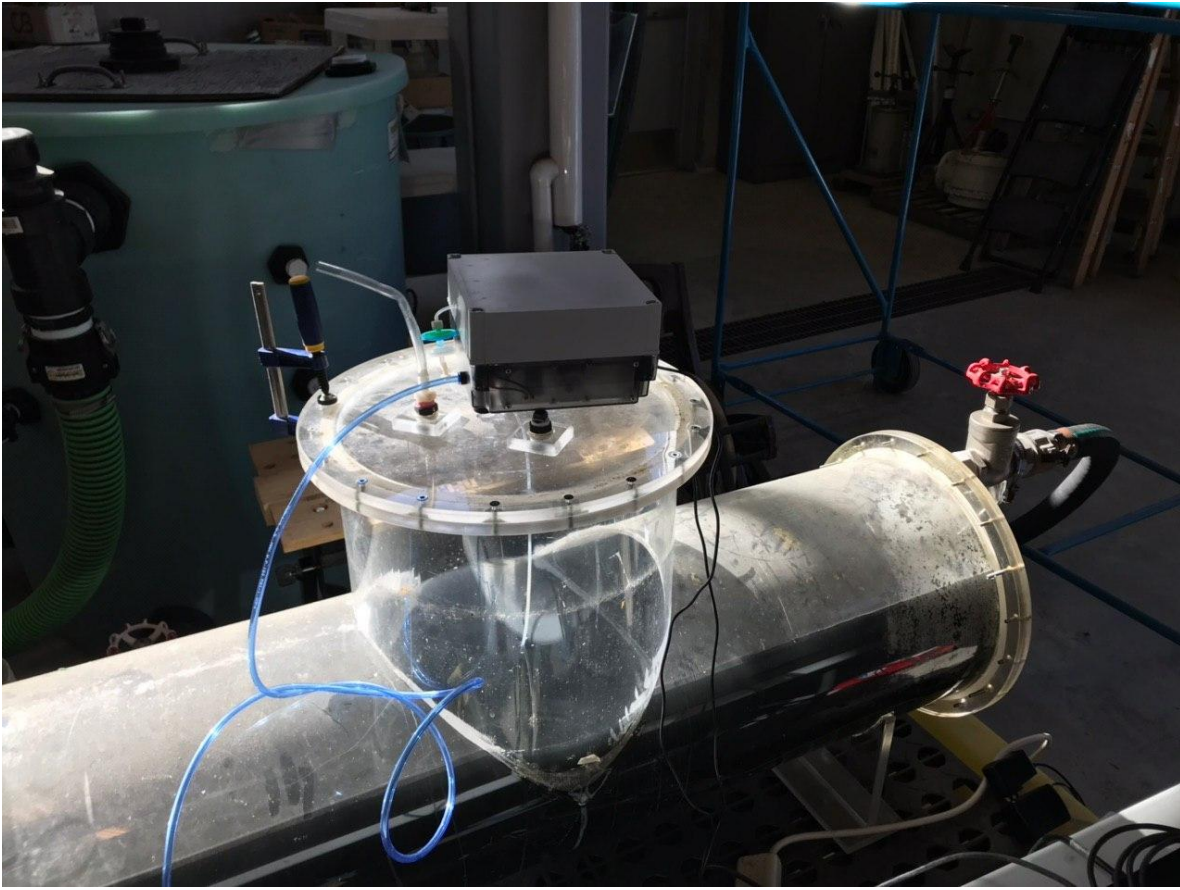


Figure 4.5 Version 2 running continuous experiments at Annacis island Research Center.

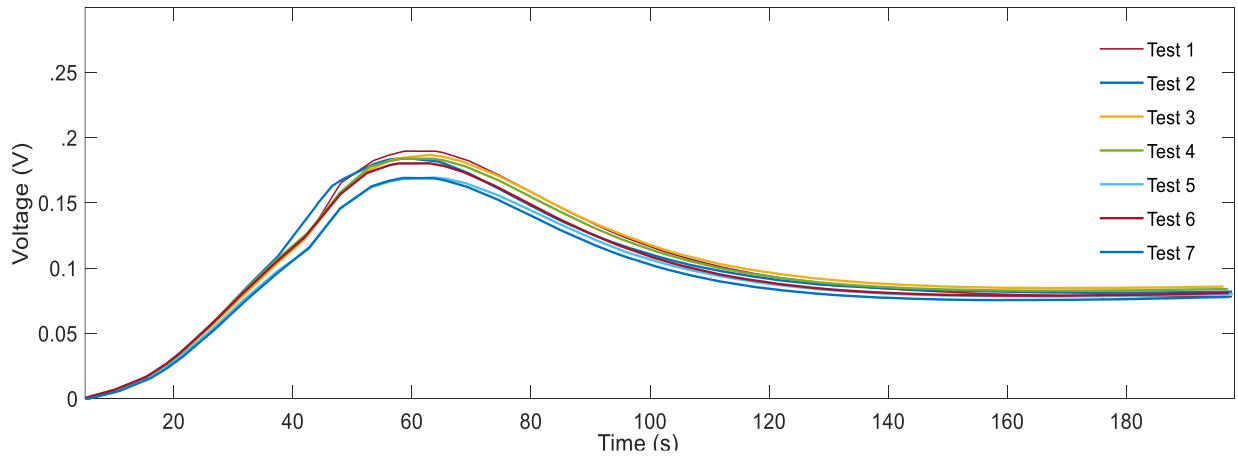


Figure 4.6 Field test responses for raw influent.

5 Summary, contributions, and future works

5.1 Summary

As a major objective of this research, a microfluidic-based detector was designed to be placed along sewer pipes for liquid phase analysis. To achieve this goal, different types of sensors were tested and the most sensitive and selective one was chosen for the detection of target compounds within the mixture of analytes available in liquid waste. Automated sample extraction and delivery system were reliably implemented in the portable setup to minimize human interactions and increase the safety of wastewater personnel. The robust platform was integrated with the control hardware to be wirelessly operated and transmit data. The developed robust platform was designed with long-lasting materials for overnight operations. The results showed that the setup collected reproducible data over long runs and was able to detect H₂S as low as 3 mg/l in aqueous solutions. Also, the detector was calibrated based on different concentrations of H₂S and NH₃ in water. The device was capable of classifying between NH₃ and H₂S by 100% and 96% recall in separate samples, and a regression precision of 84.6% was achieved. To further study the potential of the detector in mixture analysis, the sensor was exposed to the mixture of ammonia and hydrogen sulfide, and a clear distinction between these two compounds was observed (a recall of 97% for H₂S and 96% for NH₃ in classification and 88.77% precision in regression). Finally, the setup was installed in the field for continuous data collection, and it performed properly without any technical issues for over 6 hours each day.

5.2 Contributions

- (1) A microfluidic-based detector was developed for H₂S, and NH₃ detection in a mixture of analytes available in the liquid waste that can be placed along pipelines for liquid-phase analysis and thereby generation points of target gases (including noxious gases (H₂S, NH₃) dissolved in the liquid phase, can be identified which facilitates targeted treatment within the sewer network. The developed setup reduces human interactions and thereby increases the safety of wastewater treatment personnel.
- (2) Automated sample extraction and delivery system were developed and contained different stages, including sample extraction, sample filtration, vaporization of a liquid sample into a gaseous state, exposing the gases to the sensor, and purging the chambers. Control hardware to operate the detector wirelessly was implemented inside the system, and long-lasting materials suitable for operating based on the sewer environment conditions were used to fabricate the device.
- (3) The setup was calibrated against H₂S and NH₃ using standard samples, and wide concentration ranges of H₂S and NH₃ as well as influent were exposed to the microfluidic-based detector, which provided data for training and testing different machine learning models for classification and regression.

5.3 Future works

- A different sensor showing no response to water can be used within the setup to eliminate the humidity effect.

- A potentiostatic circuit can be implemented within the setup to reliably collect data using an electrochemical sensor, and the processed data can be compared with the MOS sensor results.
- An electrochemical sensor that is H₂S specific can be fabricated and implemented into the system using the portable version of potentiostat installed in the setup.

6 References

- [1] G. Jiang, J. Sun, K. R. Sharma, and Z. Yuan, “Corrosion and odor management in sewer systems,” *Curr. Opin. Biotechnol.*, vol. 33, pp. 192–197, 2015, doi: 10.1016/j.copbio.2015.03.007.
- [2] K. Park, H. Lee, S. Phelan, S. Liyanaarachchi, N. Marleni, and D. Navaratna, “Mitigation strategies of hydrogen sulphide emission in sewer networks – A review,” *Int. Biodeterior. Biodegradation*, vol. 95, pp. 251–261, Nov. 2014, doi: 10.1016/J.IBIOD.2014.02.013.
- [3] L. Zhang, P. De Schryver, B. De Gusseme, W. De Muynck, N. Boon, and W. Verstraete, “Chemical and biological technologies for hydrogen sulfide emission control in sewer systems: A review,” *Water Res.*, vol. 42, no. 1–2, pp. 1–12, Jan. 2008, doi: 10.1016/j.watres.2007.07.013.
- [4] J. S. Lim *et al.*, “SewerSnort: A drifting sensor for in situ Wastewater Collection System gas monitoring,” *Ad Hoc Networks*, vol. 11, no. 4, pp. 1456–1471, Jun. 2013, doi: 10.1016/j.adhoc.2011.01.016.
- [5] Y. Liu, K. R. Sharma, S. Murthy, I. Johnson, T. Evans, and Z. Yuan, “On-line monitoring of methane in sewer air,” *Sci. Rep.*, vol. 4, no. 1, pp. 1–8, Oct. 2014, doi: 10.1038/srep06637.
- [6] Y. Liu, K. R. Sharma, M. Fluggen, K. O’Halloran, S. Murthy, and Z. Yuan, “Online dissolved methane and total dissolved sulfide measurement in sewers,” *Water Res.*, vol.

- 68, pp. 109–118, Jan. 2015, doi: 10.1016/J.WATRES.2014.09.047.
- [7] Y. Liu, B.-J. Ni, K. R. Sharma, and Z. Yuan, “Methane emission from sewers,” *Sci. Total Environ.*, vol. 524–525, pp. 40–51, Aug. 2015, doi: 10.1016/j.scitotenv.2015.04.029.
- [8] R. O. Beauchamp, J. S. Bus, J. A. Popp, C. J. Boreiko, D. A. Andjelkovich, and P. Leber, “A critical review of the literature on hydrogen sulfide toxicity,” *Crit. Rev. Toxicol.*, vol. 13, no. 1, pp. 25–97, 1984, doi: 10.3109/10408448409029321.
- [9] L. Aventaggiato, A. P. Colucci, G. Strisciullo, F. Favalli, and R. Gagliano-Candela, “Lethal Hydrogen Sulfide poisoning in open space: An atypical case of asphyxiation of two workers,” *Forensic Sci. Int.*, vol. 308, p. 110122, Mar. 2020, doi: 10.1016/j.forsciint.2019.110122.
- [10] K. A. Brenneman, R. A. James, E. A. Gross, and D. C. Dorman, “Olfactory neuron loss in adult male CD rats following subchronic inhalation exposure to hydrogen sulfide,” *Toxicol. Pathol.*, vol. 28, no. 2, pp. 326–33, Mar. 2000, doi: 10.1177/019262330002800213.
- [11] S. Kage, H. Ikeda, N. Ikeda, A. Tsujita, and K. Kudo, “Fatal hydrogen sulfide poisoning at a dye works,” *Leg. Med.*, vol. 6, no. 3, pp. 182–186, Jul. 2004, doi: 10.1016/j.legalmed.2004.04.004.
- [12] H. S. Jensen, *Hydrogen sulfide induced concrete corrosion of sewer networks*. Institut for Kemi, Miljø og Bioteknologi, Aalborg Universitet, 2009.

- [13] J. Chen *et al.*, “Reducing H₂S production by O₂ feedback control during large-scale sewage sludge composting,” *Waste Manag.*, vol. 31, no. 1, pp. 65–70, Jan. 2011, doi: 10.1016/j.wasman.2010.08.020.
- [14] J. Arogo, R. H. Zhang, G. L. Riskowski, and D. L. Day, “HYDROGEN SULFIDE PRODUCTION FROM STORED LIQUID SWINE MANURE: A LABORATORY STUDY,” *Trans. ASAE*, vol. 43, no. 5, pp. 1241–1245, Sep. 2000, doi: 10.13031/2013.3017.
- [15] M. Mahmoodian and A. M. Alani, “Effect of Temperature and Acidity of Sulfuric Acid on Concrete Properties,” *J. Mater. Civ. Eng.*, vol. 29, no. 10, p. 04017154, Oct. 2017, doi: 10.1061/(ASCE)MT.1943-5533.0002002.
- [16] M. O’Connell, C. McNally, and M. G. Richardson, “Biochemical attack on concrete in wastewater applications: A state of the art review,” *Cem. Concr. Compos.*, vol. 32, no. 7, pp. 479–485, Aug. 2010, doi: 10.1016/j.cemconcomp.2010.05.001.
- [17] D. Trejo, P. De Figueiredo, M. Sanchez, C. Gonzalez, S. Wei, and L. Li, “ANALYSIS AND ASSESSMENT OF MICROBIAL BIOFILM-MEDIATED CONCRETE DETERIORATION 5. Report Date 13. Type of Report and Period Covered Unclassified,” Southwest Region University Transportation Center (U.S.), Oct. 1700.
- [18] S. Wei, M. Sanchez, D. Trejo, and C. Gillis, “Microbial mediated deterioration of reinforced concrete structures,” *Int. Biodeterior. Biodegrad.*, vol. 64, no. 8, pp. 748–754, Dec. 2010, doi: 10.1016/j.ibiod.2010.09.001.

- [19] T. Wells, R. E. Melchers, and P. Bond, “Factors involved in the long term corrosion of concrete sewers,” *49th Annu. Conf. Australas. Corros. Assoc. 2009 Corros. Prev. 2009*, Jan. 2009.
- [20] A. C. D. Parker, “Mechanics of Corrosion of Concrete Sewers by Hydrogen Sulfide MECHANICS OF CORROSION OF CONCRETE BY HYDROGEN SULFIDE * By,” vol. 23, no. 12, pp. 1477–1485, 2011.
- [21] M. G. D. Gutiérrez-Padilla, A. Bielefeldt, S. Ovtchinnikov, M. Hernandez, and J. Silverstein, “Biogenic sulfuric acid attack on different types of commercially produced concrete sewer pipes,” *Cem. Concr. Res.*, vol. 40, no. 2, pp. 293–301, Feb. 2010, doi: 10.1016/j.cemconres.2009.10.002.
- [22] T. Hvitved-Jacobsen, J. Vollertsen, and J. S. Matos, “The sewer as a bioreactor--a dry weather approach.,” *Water Sci. Technol. a J. Int. Assoc. Water Pollut. Res.*, vol. 45, no. 3, pp. 11–24, 2002.
- [23] P. L. Ng and A. K. H. Kwan, “Improving concrete durability for sewerage applications,” *Lect. Notes Mech. Eng.*, vol. 19, pp. 1043–1053, 2015, doi: 10.1007/978-3-319-09507-3_89.
- [24] B. Burton, L. Gu, and Y. Y. Yin, “Overview of Vulnerabilities of Coastally-Influenced Conveyance and Treatment Infrastructure in Greater Vancouver to Climate Change: Identification of Adaptive Responses,” in *Impacts of Global Climate Change*, 2005, pp. 1–12, doi: 10.1061/40792(173)79.

- [25] V. Baskar, "Research and evaluate the use of wastewater contaminant fees," pp. 1–168, 2019.
- [26] R. Preetham, R. Hari Krishna, M. N. Chandraprabha, and T. Thomas, "Vehicular soot for improvement of chemical stability of cement composites towards acid rain and sewage like atmospheres," *Constr. Build. Mater.*, vol. 248, p. 118604, Jul. 2020, doi: 10.1016/j.conbuildmat.2020.118604.
- [27] N. De Belie, J. Monteny, A. Beeldens, E. Vincke, D. Van Gemert, and W. Verstraete, "Experimental research and prediction of the effect of chemical and biogenic sulfuric acid on different types of commercially produced concrete sewer pipes," *Cem. Concr. Res.*, vol. 34, no. 12, pp. 2223–2236, Dec. 2004, doi: 10.1016/j.cemconres.2004.02.015.
- [28] V. B. Møller, K. Dam-Johansen, S. M. Frankær, and S. Kiil, "Acid-resistant organic coatings for the chemical industry: a review," *J. Coatings Technol. Res.*, vol. 14, no. 2, pp. 279–306, 2017.
- [29] F. Eiwien, J.-H. Pfeiler, and C. Roos, "Corrosion resistance of CaO–Al₂O₃–SiO₂ glasses used for flame spraying on concrete," *Phys. Chem. Glas. Eur. J. Glas. Sci. Technol. Part B*, vol. 61, no. 1, pp. 11–20, Feb. 2020, doi: 10.13036/17533562.61.1.05.
- [30] J. M. Estrada, N. J. R. B. Kraakman, R. Muñoz, and R. Lebrero, "A comparative analysis of odour treatment technologies in wastewater treatment plants," *Environ. Sci. Technol.*, vol. 45, no. 3, pp. 1100–1106, Feb. 2011, doi: 10.1021/es103478j.
- [31] F. Fan, R. Xu, D. Wang, and F. Meng, "Application of activated sludge for odor control in

- wastewater treatment plants: Approaches, advances and outlooks,” *Water Research*, vol. 181. Elsevier Ltd, p. 115915, 15-Aug-2020, doi: 10.1016/j.watres.2020.115915.
- [32] C. Grengg, F. Mittermayr, N. Ukrainczyk, G. Koraimann, S. Kienesberger, and M. Dietzel, “Advances in concrete materials for sewer systems affected by microbial induced concrete corrosion: A review,” *Water Res.*, vol. 134, pp. 341–352, 2018.
- [33] L. Gu, P. Visintin, and T. Bennett, “Sulphuric Acid Resistance of Cementitious Materials: Multiscale Approach to Assessing the Degradation,” *J. Mater. Civ. Eng.*, vol. 32, no. 7, p. 04020171, Jul. 2020, doi: 10.1061/(ASCE)MT.1943-5533.0003261.
- [34] X. Li *et al.*, “Increased Resistance of Nitrite-Admixed Concrete to Microbially Induced Corrosion in Real Sewers,” *Environ. Sci. Technol.*, vol. 54, no. 4, pp. 2323–2333, Feb. 2020, doi: 10.1021/acs.est.9b06680.
- [35] A. H. Nielsen, T. Hvitved-Jacobsen, and J. Vollertsen, “Recent findings on sinks for sulfide in gravity sewer networks,” *Water Sci. Technol.*, vol. 54, no. 6–7, pp. 127–134, Sep. 2006, doi: 10.2166/wst.2006.578.
- [36] K. Park *et al.*, “Mitigation strategies of hydrogen sulphide emission in sewer networks - A review,” *Int. Biodeterior. Biodegrad.*, vol. 95, no. PA, pp. 251–261, Nov. 2014, doi: 10.1016/j.ibiod.2014.02.013.
- [37] I. I. N. Etim *et al.*, “Mitigation of sulphate-reducing bacteria attack on the corrosion of 20SiMn steel rebar in sulphotoaluminate concrete using organic silicon quaternary ammonium salt,” *Constr. Build. Mater.*, vol. 257, p. 119047, Oct. 2020, doi:

10.1016/j.conbuildmat.2020.119047.

- [38] U. S. EPA, “Hydrogen sulfide corrosion in wastewater collection and treatment system,” 1991.
- [39] T. Ochi, M. Kitagawa, and S. Tanaka, “Controlling sulfide generation in force mains by air injection,” *Water Sci. Technol.*, vol. 37, no. 1, pp. 87–95, Jan. 1998, doi: 10.2166/wst.1998.0022.
- [40] N. Tanaka and K. Takenaka, “Control of hydrogen sulfide and degradation of organic matter by air injection into a wastewater force main,” *Water Sci. Technol.*, vol. 31, no. 7, pp. 273–282, Apr. 1995, doi: 10.2166/wst.1995.0243.
- [41] G. H. Chen and D. H. W. Leung, “Utilization of oxygen in a sanitary gravity sewer,” *Water Res.*, vol. 34, no. 15, pp. 3813–3821, Oct. 2000, doi: 10.1016/S0043-1354(00)00143-3.
- [42] S. Delgado, M. Alvarez, E. Aguiar, and L. E. Rodríguez-Gómez, “Effect of dissolved oxygen in reclaimed wastewater transformation during transportation. Case study: Tenerife, Spain,” *Water Sci. Technol.*, vol. 37, no. 1, pp. 123–130, Jan. 1998, doi: 10.2166/wst.1998.0030.
- [43] R. P. G. Bowker, G. A. Audibert, H. J. Shah, and N. A. Webster, “Detection, control, and correction of hydrogen sulfide corrosion in existing wastewater systems,” *Off. Wastewater Enforc. Compliance, Off. Water, Washington, DC*, 1992.

- [44] M. Tomar and T. H. A. Abdullah, "Evaluation of chemicals to control the generation of malodorous hydrogen sulfide in waste water," *Water Res.*, vol. 28, no. 12, pp. 2545–2552, 1994.
- [45] W. Yang, J. Vollertsen, and T. Hvitved-Jacobsen, "Anoxic sulfide oxidation in wastewater of sewer networks," *Water Sci. Technol.*, vol. 52, no. 3, pp. 191–199, 2005.
- [46] ASCE, "Sulfide in wastewater collection and treatment systems," *Manuals and reports on engineering practice No. 69*. 1989.
- [47] P. Jameel, "The use of ferrous chloride to control dissolved sulfides in interceptor sewers," *J. (Water Pollut. Control Fed.)*, pp. 230–236, 1989.
- [48] A. H. Nielsen, P. Lens, J. Vollertsen, and T. Hvitved-Jacobsen, "Sulfide–iron interactions in domestic wastewater from a gravity sewer," *Water Res.*, vol. 39, no. 12, pp. 2747–2755, 2005.
- [49] R. D. Pomeroy, *Process design manual for sulfide control in sanitary sewerage systems*. US Environmental Protection Agency, Technology Transfer, 1974.
- [50] N. A. Padival, J. S. Weiss, and R. G. Arnold, "Control of Thiobacillus by means of microbial competition: implications for corrosion of concrete sewers," *Water Environ. Res.*, vol. 67, no. 2, pp. 201–205, 1995.
- [51] A. Jayaraman, F. B. Mansfeld, and T. K. Wood, "Inhibiting sulfate-reducing bacteria in biofilms by expressing the antimicrobial peptides indolicidin and bactenecin," *J. Ind.*

- Microbiol. Biotechnol.*, vol. 22, no. 3, pp. 167–175, 1999.
- [52] M. Nemati, T. J. Mazutinec, G. E. Jenneman, and G. Voordouw, “Control of biogenic H₂S production with nitrite and molybdate,” *J. Ind. Microbiol. Biotechnol.*, vol. 26, no. 6, pp. 350–355, 2001.
- [53] M. A. Reinsel, J. T. Sears, P. S. Stewart, and M. J. McInerney, “Control of microbial souring by nitrate, nitrite or glutaraldehyde injection in a sandstone column,” *J. Ind. Microbiol.*, vol. 17, no. 2, pp. 128–136, 1996.
- [54] F. I. M. Ali, F. Awwad, Y. E. Greish, and S. T. Mahmoud, “Hydrogen Sulfide (H₂S) Gas Sensor: A Review,” *IEEE Sens. J.*, vol. 19, no. 7, pp. 2394–2407, Apr. 2019, doi: 10.1109/JSEN.2018.2886131.
- [55] S. K. Pandey, K.-H. Kim, and K.-T. Tang, “A review of sensor-based methods for monitoring hydrogen sulfide,” *TrAC Trends Anal. Chem.*, vol. 32, pp. 87–99, Feb. 2012, doi: 10.1016/j.trac.2011.08.008.
- [56] A. Scozzari, “Electrochemical sensing methods: A brief review,” in *NATO Security through Science Series C: Environmental Security*, 2008, pp. 335–352, doi: 10.1007/978-1-4020-8480-5_16.
- [57] W. Yourong, Y. Heqing, and W. E’feng, “The electrochemical oxidation and the quantitative determination of hydrogen sulfide on a solid polymer electrolyte-based system,” *J. Electroanal. Chem.*, vol. 497, no. 1–2, pp. 163–167, Feb. 2001, doi: 10.1016/S0022-0728(00)00449-6.

- [58] X. Liang *et al.*, “Solid-state potentiometric H₂S sensor combining NASICON with Pr₆O₁₁-doped SnO₂ electrode,” *Sensors Actuators, B Chem.*, vol. 125, no. 2, pp. 544–549, Aug. 2007, doi: 10.1016/j.snb.2007.02.050.
- [59] C. Yu, Y. Wang, K. Hua, W. Xing, and T. Lu, “Electrochemical H₂S sensor with H₂SO₄ pre-treated Nafion membrane as solid polymer electrolyte,” *Sensors Actuators, B Chem.*, vol. 86, no. 2–3, pp. 259–265, Sep. 2002, doi: 10.1016/S0925-4005(02)00200-9.
- [60] M. Taillefert, G. W. Luther III, and D. B. Nuzzio, “The application of electrochemical tools for in situ measurements in aquatic systems,” *Electroanal. An Int. J. Devoted to Fundam. Pract. Asp. Electroanal.*, vol. 12, no. 6, pp. 401–412, 2000.
- [61] B. Spilker, J. Randhahn, H. Grabow, H. Beikirch, and P. Jeroschewski, “New electrochemical sensor for the detection of hydrogen sulfide and other redox active species,” *J. Electroanal. Chem.*, vol. 612, no. 1, pp. 121–130, Jan. 2008, doi: 10.1016/j.jelechem.2007.09.019.
- [62] J. Flávio da Silveira Petrucci *et al.*, “Monitoring of hydrogen sulfide via substrate-integrated hollow waveguide mid-infrared sensors in real-time,” *Analyst*, vol. 139, no. 1, pp. 198–203, Nov. 2014, doi: 10.1039/c3an01793a.
- [63] E. A. Guenther, K. S. Johnson, and K. H. Coale, “Direct ultraviolet spectrophotometric determination of total sulfide and iodide in natural waters,” *Anal. Chem.*, vol. 73, no. 14, pp. 3481–3487, Jul. 2001, doi: 10.1021/ac0013812.
- [64] *Laser in Environmental and Life Sciences*. Springer Berlin Heidelberg, 2004.

- [65] C. Oppenheimer, P. Francis, M. Burton, A. J. H. Maciejewski, and L. Boardman, "Remote measurement of volcanic gases by Fourier transform infrared spectroscopy," *Appl. Phys. B Lasers Opt.*, vol. 67, no. 4, pp. 505–515, 1998, doi: 10.1007/s003400050536.
- [66] J. Y. Wong and R. L. Anderson, *Non-dispersive infrared gas measurement*. Lulu. com, 2012.
- [67] A. Varga, Z. Bozóki, M. Szakáll, and G. Szabó, "Photoacoustic system for on-line process monitoring of hydrogen sulfide (H₂S) concentration in natural gas streams," *Appl. Phys. B Lasers Opt.*, vol. 85, no. 2–3, pp. 315–321, Nov. 2006, doi: 10.1007/s00340-006-2388-6.
- [68] X. Jiang, K. Kim, S. Zhang, J. Johnson, and G. Salazar, "High-Temperature Piezoelectric Sensing," *Sensors*, vol. 14, no. 1, pp. 144–169, Dec. 2013, doi: 10.3390/s140100144.
- [69] M. T. S. R. Gomes, P. S. T. Nogueira, and J. A. B. P. Oliveira, "Quantification of CO₂, SO₂, NH₃, and H₂S with a single coated piezoelectric quartz crystal," *Sensors Actuators, B Chem.*, vol. 68, no. 1, pp. 218–222, Aug. 2000, doi: 10.1016/S0925-4005(00)00432-9.
- [70] W. P. Jakubik, M. Urbanczyk, E. Maciak, T. Pustelny, and A. Stolarczyk, "Polyaniline thin films as a toxic gas sensors in SAW system*," *J. Phys. IV*, vol. 129, pp. 121–124, Oct. 2005, doi: 10.1051/jp4:2005129026.
- [71] M. Kaur *et al.*, "Room-temperature H₂S gas sensing at ppb level by single crystal In₂O₃ whiskers," *Sensors Actuators, B Chem.*, vol. 133, no. 2, pp. 456–461, Aug. 2008, doi: 10.1016/j.snb.2008.03.003.

- [72] D. D. Vuong, G. Sakai, K. Shimanoe, and N. Yamazoe, "Hydrogen sulfide gas sensing properties of thin films derived from SnO₂ sols different in grain size," *Sensors Actuators, B Chem.*, vol. 105, no. 2, pp. 437–442, Mar. 2005, doi: 10.1016/j.snb.2004.06.034.
- [73] C. M. Ghimbeu, M. Lumbreras, M. Siadat, R. C. van Landschoot, and J. Schoonman, "Electrostatic sprayed SnO₂ and Cu-doped SnO₂ films for H₂S detection," *Sensors Actuators, B Chem.*, vol. 133, no. 2, pp. 694–698, Aug. 2008, doi: 10.1016/j.snb.2008.04.007.
- [74] J. Gong, Q. Chen, M. R. Lian, N. C. Liu, R. G. Stevenson, and F. Adami, "Micromachined nanocrystalline silver doped SnO₂ H₂S sensor," *Sensors Actuators, B Chem.*, vol. 114, no. 1, pp. 32–39, Mar. 2006, doi: 10.1016/j.snb.2005.04.035.
- [75] S. Sen *et al.*, "Highly sensitive hydrogen sulphide sensors operable at room temperature," *Sensors Actuators, B Chem.*, vol. 115, no. 1, pp. 270–275, May 2006, doi: 10.1016/j.snb.2005.09.013.
- [76] H. M. Lin, C. M. Hsu, H. Y. Yang, P. Y. Lee, and C. C. Yang, "Nanocrystalline WO₃-based H₂S sensors," *Sensors Actuators B. Chem.*, vol. 22, no. 1, pp. 63–68, Oct. 1994, doi: 10.1016/0925-4005(94)01256-3.
- [77] W. H. Tao and C. H. Tsai, "H₂S sensing properties of noble metal doped WO₃ thin film sensor fabricated by micromachining," *Sensors Actuators, B Chem.*, vol. 81, no. 2–3, pp. 237–247, Jan. 2002, doi: 10.1016/S0925-4005(01)00958-3.

- [78] K. Gupta, H. Choo, H. Kim, and R. S. Muller, "Micromachined polarization beam splitters for the visible spectrum," in *2003 IEEE/LEOS International Conference on Optical MEMS (Cat. No.03EX682)*, 2003, pp. 171–172, doi: 10.1109/OMEMS.2003.1233520.
- [79] A. Ebrahimi, A. Pirouz, Y. Abdi, S. Azimi, and S. Mohajerzadeh, "Selective deposition of CuO/SnO₂ sol-gel on porous SiO₂ suitable for the fabrication of MEMS-based H₂S sensors," *Sensors Actuators, B Chem.*, vol. 173, pp. 802–810, Oct. 2012, doi: 10.1016/j.snb.2012.07.104.
- [80] B. Urasinska-Wojcik and J. W. Gardner, "Identification of H₂S Impurity in Hydrogen Using Temperature Modulated Metal Oxide Resistive Sensors with a Novel Signal Processing Technique," *IEEE Sensors Lett.*, vol. 1, no. 4, pp. 1–4, Jun. 2017, doi: 10.1109/lsens.2017.2709345.
- [81] S. Kanan, O. El-Kadri, I. Abu-Yousef, and M. Kanan, "Semiconducting Metal Oxide Based Sensors for Selective Gas Pollutant Detection," *Sensors*, vol. 9, no. 10, pp. 8158–8196, Oct. 2009, doi: 10.3390/s91008158.
- [82] C. S. Rout, M. Hegde, and C. N. R. Rao, "H₂S sensors based on tungsten oxide nanostructures," *Sensors Actuators, B Chem.*, vol. 128, no. 2, pp. 488–493, Jan. 2008, doi: 10.1016/j.snb.2007.07.013.
- [83] A. I. Ayeshe, A. F. S. Abu-Hani, S. T. Mahmoud, and Y. Haik, "Selective H₂S sensor based on CuO nanoparticles embedded in organic membranes," *Sensors Actuators, B Chem.*, vol. 231, pp. 593–600, Aug. 2016, doi: 10.1016/j.snb.2016.03.078.

- [84] A. F. S. Abu-Hani, F. Awwad, Y. E. Greish, A. I. Ayeshe, and S. T. Mahmoud, "Design, fabrication, and characterization of low-power gas sensors based on organic-inorganic nano-composite," *Org. Electron.*, vol. 42, pp. 284–292, Mar. 2017, doi: 10.1016/j.orgel.2016.12.050.
- [85] K. Maebashi *et al.*, "Toxicological analysis of 17 autopsy cases of hydrogen sulfide poisoning resulting from the inhalation of intentionally generated hydrogen sulfide gas," *Forensic Sci. Int.*, vol. 207, no. 1–3, pp. 91–95, Apr. 2011, doi: 10.1016/j.forsciint.2010.09.008.
- [86] V. Vitvitsky and R. Banerjee, "H₂S analysis in biological samples using gas chromatography with sulfur chemiluminescence detection," in *Methods in Enzymology*, vol. 554, Academic Press Inc., 2015, pp. 111–123.
- [87] R. M. Stuetz, R. A. Fenner, and G. Engin, "Assessment of odours from sewage treatment works by an electronic nose, H₂S analysis and olfactometry," *Water Res.*, vol. 33, no. 2, pp. 453–461, Feb. 1999, doi: 10.1016/S0043-1354(98)00246-2.
- [88] C. Pace, W. Khalaf, M. Latino, N. Donato, and G. Neri, "E-nose Development for Safety Monitoring Applications in Refinery Environment," *Procedia Eng.*, vol. 47, pp. 1267–1270, Jan. 2012, doi: 10.1016/j.proeng.2012.09.384.
- [89] S. Rahman *et al.*, "Wireless E-Nose Sensors to Detect Volatile Organic Gases through Multivariate Analysis," *Micromachines*, vol. 11, no. 6, p. 597, Jun. 2020, doi: 10.3390/mi11060597.

- [90] S.-J. Ryu, E. Arifin, S.-W. Ha, and J.-K. Lee, “On-site Colorimetric Forensic Sensor (I): Quantitative Detection of Toxic H₂S and NH₃ Gases Using Metal-Ion-modified Silica Powders,” *Bull. Korean Chem. Soc.*, vol. 36, no. 10, pp. 2434–2439, Oct. 2015, doi: 10.1002/bkcs.10466.
- [91] K. Toda, P. K. Dasgupta, J. Li, G. A. Tarver, and G. M. Zarus, “Fluorometric field instrument for continuous measurement of atmospheric hydrogen sulfide,” *Anal. Chem.*, vol. 73, no. 23, pp. 5716–5724, Dec. 2001, doi: 10.1021/ac010602g.
- [92] A. B. Bluhme, J. L. Ingemar, C. Meusinger, and M. S. Johnson, “Water vapor inhibits hydrogen sulfide detection in pulsed fluorescence sulfur monitors,” *Atmos. Meas. Tech.*, vol. 9, no. 6, pp. 2669–2673, Jun. 2016, doi: 10.5194/amt-9-2669-2016.
- [93] K. Toda, S. I. Ohira, T. Tanaka, T. Nishimura, and P. K. Dasgupta, “Field Instrument for Simultaneous Large Dynamic Range Measurement of Atmospheric Hydrogen Sulfide, Methanethiol, and Sulfur Dioxide,” *Environ. Sci. Technol.*, vol. 38, no. 5, pp. 1529–1536, Mar. 2004, doi: 10.1021/es034450d.
- [94] S. I. Ohira and K. Toda, “Micro gas analysis system for measurement of atmospheric hydrogen sulfide and sulfur dioxide,” *Lab Chip*, vol. 5, no. 12, pp. 1374–1379, Nov. 2005, doi: 10.1039/b511281h.
- [95] S. I. Ohira and K. Toda, “Micro gas analyzers for environmental and medical applications,” *Analytica Chimica Acta*, vol. 619, no. 2. Elsevier, pp. 143–156, 07-Jul-2008, doi: 10.1016/j.aca.2008.05.010.

- [96] X. Qin, W. Feng, X. Yang, J. Wei, and G. Huang, "Molybdenum sulfide/citric acid composite membrane-coated long period fiber grating sensor for measuring trace hydrogen sulfide gas," *Sensors Actuators, B Chem.*, vol. 272, pp. 60–68, Nov. 2018, doi: 10.1016/j.snb.2018.05.152.
- [97] J. F. D. S. Petrucci and A. A. Cardoso, "Sensitive luminescent paper-based sensor for the determination of gaseous hydrogen sulfide," *Anal. Methods*, vol. 7, no. 6, pp. 2687–2692, Mar. 2015, doi: 10.1039/c4ay02952f.
- [98] Y. Teng *et al.*, "A spendable gas sensor with higher sensitivity and lowest detection limit towards H₂S: Porous α -Fe₂O₃ hierarchical tubule derived from poplar branch," *Chem. Eng. J.*, vol. 392, p. 123679, Jul. 2020, doi: 10.1016/j.cej.2019.123679.
- [99] J. Čmelík, J. Machát, V. Otruba, and V. Kanický, "Contribution to vapor generation-inductively coupled plasma spectrometric techniques for determination of sulfide in water samples," *Talanta*, vol. 80, no. 5, pp. 1777–1781, Mar. 2010, doi: 10.1016/j.talanta.2009.10.022.
- [100] M. Colon, J. L. Todolí, M. Hidalgo, and M. Iglesias, "Development of novel and sensitive methods for the determination of sulfide in aqueous samples by hydrogen sulfide generation-inductively coupled plasma-atomic emission spectroscopy," *Anal. Chim. Acta*, vol. 609, no. 2, pp. 160–168, Feb. 2008, doi: 10.1016/j.aca.2008.01.001.
- [101] B. Tan *et al.*, "New method for quantification of gasotransmitter hydrogen sulfide in biological matrices by LC-MS/MS," *Sci. Rep.*, vol. 7, no. 1, pp. 1–12, Apr. 2017, doi:

10.1038/srep46278.

- [102] S. Youssef, S. Zhang, and H. W. Ai, “A Genetically Encoded, Ratiometric Fluorescent Biosensor for Hydrogen Sulfide,” *ACS Sensors*, vol. 4, no. 6, pp. 1626–1632, Jun. 2019, doi: 10.1021/acssensors.9b00400.
- [103] M. Hanada *et al.*, “Portable oral malodor analyzer using highly sensitive In₂O₃ gas sensor combined with a simple gas chromatography system,” *Anal. Chim. Acta*, vol. 475, no. 1–2, pp. 27–35, Jan. 2003, doi: 10.1016/S0003-2670(02)01038-3.
- [104] Thermo Scientific™, “Hydrogen Sulfide - Sulfur Dioxide Analyzer Model 450.” [Online]. Available: <https://www.thermofisher.com/order/catalog/product/450I#/450I>. [Accessed: 17-Aug-2020].
- [105] Y. Liu, K. R. Sharma, M. Fluggen, K. O’Halloran, S. Murthy, and Z. Yuan, “Online dissolved methane and total dissolved sulfide measurement in sewers,” *Water Res.*, vol. 68, pp. 109–118, Jan. 2015, doi: 10.1016/j.watres.2014.09.047.
- [106] M. Paknahad, J. S. Bachhal, A. Ahmadi, and M. Hoorfar, “Characterization of channel coating and dimensions of microfluidic-based gas detectors,” *Sensors Actuators B Chem.*, vol. 241, pp. 55–64, Mar. 2017, doi: 10.1016/j.snb.2016.10.048.
- [107] M. M. Montazeri, N. De Vries, A. D. Afantchao, A. O’Brien, P. Kadota, and M. Hoorfar, “Development of a Sensing Platform for Nuisance Sewer Gas Monitoring: Hydrogen Sulfide Detection in Aqueous Versus Gaseous Samples,” *IEEE Sens. J.*, vol. 18, no. 19, pp. 7772–7778, Oct. 2018, doi: 10.1109/JSEN.2018.2866305.

- [108] M. Paknahad, J. S. Bachhal, and M. Hoorfar, “Diffusion-based humidity control membrane for microfluidic-based gas detectors,” *Anal. Chim. Acta*, vol. 1021, pp. 103–112, Aug. 2018, doi: 10.1016/j.aca.2018.03.021.